REPORT 1205

A WIND-TUNNEL INVESTIGATION OF THE EFFECTS OF THRUST-AXIS INCLINATION ON PROPELLER FIRST-ORDER VIBRATION [1]

By W. H. GRAY, J. M. HALLISSY, JR.,
and A. R. HEATH, JR.

SUMMARY

Data on the aerodynamic excitation of first-order vibration occurring in a representative three-blade propeller having its thrust axis inclined to the airstream at angles of 0°, 4.55°, and 9.80° are included in this report. For several representative conditions the aerodynamic excitation has been computed and compared with the measured values. Blade stresses also were measured to permit the evaluation of the blade stress resulting from a given blade aerodynamic excitation.

It was concluded that the section aerodynamic exciting force of a pitched propeller may be computed accurately at low rotational speeds. As section velocities approach the speed of sound, the accuracy of computation of section aerodynamic exciting force is not always so satisfactory.

The first-order vibratory stress was proportional to the product of thrust-axis inclination and dynamic pressure at low rotational speeds. The stresses at the high rotational speeds were lower than would be anticipated if the stresses were estimated by extrapolation of the low-rotational-speed stresses. A stress prediction which assumed a linear relation between first-order vibratory stress and the product of pitch angle and dynamic pressure and which was based on stresses at low rotational speeds was conservative for these blades when the outer portions of the blade are in the transonic and low supersonic speed range.

INTRODUCTION

Propeller vibration arising from inclination of the thrust axis relative to the airstream has recently become an important problem. The vibration occurs because each blade section operates at a varying angle of attack and Mach number as it rotates and, consequently, causes fluctuating lift forces which complete an excitation cycle once each revolution. Modern airplane-design trends toward higher wing loading, higher speed, and longer range have increased the magnitude of the change of propeller inflow angle from take-off with maximum wing loading to the condition of high speed and minimum wing loading. The total angle change for a given airplane may be as small as 10° or as great as 30°, and the resulting stresses may be excessively high even though resonance is not attained. The problem has been further aggravated by the need for thin propeller blade sections for high speed airplanes utilizing gas-turbine power plants.

Much has been written on the subject of propeller aerodynamic excitation resulting from eccentric loading, and numerous methods for relieving blade stress caused by this type of vibration have been proposed or tried. Until recently, however, even an adequate theory for predicting the exciting force has been lacking, and no quantitative stress measurements were obtained under closely controlled testing conditions. In view of the seriousness of the problem, a broad research program has been undertaken to include:

(1) Tests of a tilted propeller in a uniform flow stream at subsonic and supersonic section speeds

(2) Full-scale tests with a wing-fuselage-propeller combination to determine interference effects (ref. 1)

(3) The establishment of an adequate method of calculating the fluctuating aerodynamic loads (ref. 2)

This report covers part (1) of this program. The fluctuating aerodynamic loads have been measured by slipstream surveys and are compared with calculated values for the same conditions. In addition, stress measurements have been made on the blades and the results are compared with calculated stresses.

SYMBOLS

a	slope of lift curve per degree, $dc_l/d\alpha$
b	blade width, ft
C_T	thrust coefficient, $T/\rho n^2 D^4$
C_T'	blade-section thrust coefficient, dC_T/dx
$C_T'_{\omega t}$	instantaneous blade-section thrust coefficient
$C_T'_{\omega t(corr)}$	instantaneous blade-section thrust coefficient corrected to propeller rotational speed
c_l	section lift coefficient
c_{l_d}	design section lift coefficient
D	propeller diameter, ft
f	natural frequency of rotating propeller blade, cps
f_0	static natural frequency of propeller blade, cps
h	blade-section maximum thickness, ft
J	advance ratio, V/nD
$J_{\omega t}$	instantaneous advance ratio
N	propeller rotational speed, rpm
n	propeller rotational speed, rps
$n_{\omega t}$	apparent instantaneous propeller rotational speed, rps

q	free-stream dynamic pressure, $\frac{1}{2}\rho V^2$, lb/sq ft
R	propeller tip radius, ft
r	radius to a blade section, ft
T	thrust, lb
t	time, sec
V	airspeed, fps
W	resultant velocity at blade section, fps
$W_{\omega t}$	instantaneous resultant velocity at blade section, fps
x	fraction of propeller tip radius, r/R
α	section angle of attack, deg
α_T	angle of thrust axis with respect to airstream (inflow angle), deg
β	blade angle, deg
ρ	mass density of air, slugs/cu ft
ϕ_0	geometric helix angle, $\tan^{-1}\dfrac{J}{\pi x}$, deg
$\phi_{0\omega t}$	instantaneous geometric helix angle,

$$\tan^{-1}\frac{\cos\alpha_T}{\dfrac{\pi x}{J}+\sin\alpha_T\sin\omega t},\ \text{deg}$$

ω	angular velocity of propeller, deg/sec

APPARATUS

PROPELLER DYNAMOMETER

The Langley 2,000-horsepower propeller dynamometer was used for these tests with certain minor alterations necessary for operation of the propeller with the thrust axis in a pitched position. Pitching of the propeller axis was accomplished by inserting wedges of the desired angles between the base of the dynamometer support strut and the tunnel floor. A nose-down position was employed and the propeller center was retained approximately at the center line of the tunnel. A sketch of the dynamometer mounted in the Langley 16-foot high-speed tunnel is shown in figure 1.

WAKE-SURVEY RAKE

A survey rake containing 27 total-pressure tubes was used to obtain wake data. Figure 2 shows the survey strut installed in the test section. The rake was supported at one end by the dynamometer nose fairing and at the other end by the tunnel wall, with mounting provisions for six angular locations behind the propeller. The mountings were so arranged that the rake tubes were alined parallel to the tunnel axis.

By use of the convention that 0° is in the direction of axis inclination, or bottom center in this case, the angular strut locations chosen were 75°, 105°, 150°, 255°, 285°, and 330° as measured in the direction of rotation. It was anticipated that the maximum blade loading would occur near 90° and the minimum blade loading near 270°. The choice of strut positions was made in order to fix as nearly as possible the position and magnitude of the maximum and minimum blade loadings.

PROPELLER

A three-blade propeller utilizing NACA 10–(3)(08)–03 solid aluminum-alloy blades, with NACA 16-series sections, mounted in a three-way adjustable-blade hub was employed for most of the tests. The blade-form curves, design blade-angle curve, and plan form for this blade are shown in figure 3. Some tests were also made with a two-blade propeller employing blades of the same design mounted in a similar four-way hub. In addition, a few tests were made with the same blades mounted in a semiarticulated propeller hub. Figure 4 is a sketch of this hub. As can be seen, the two blades are rigidly connected to each other but are able to rotate as a unit about an axis which is perpendicular to and intersects both the propeller shaft axis and the blade axes. The motion is unrestrained within a limit of about 5° each way from the center position.

INSTRUMENTATION

Wire strain gages were used to measure blade stresses and, in all cases, were mounted on the cambered surfaces of the blades. Vibratory stresses were measured with Baldwin SR–4 type C strain gages and steady stress was measured with a single group of type A strain gages installed on a separate blade.

A schematic drawing of the wiring arrangement is shown in figure 5. Bridge circuits were used in connecting the gages and, in order to avoid temperature-compensation difficulties, each bridge was made up completely of strain gages mounted on the blade at the point where a stress measurement was desired. The two gages used as the active arms of each bridge were mounted side by side, parallel to the blade axis, and centered about the nominal location. The two gages used as the dummy arms of each bridge were mounted perpendicular to the blade axis and adjacent to the active-arm gages. The bridge outputs were transmitted through a slip-ring device, or "pineapple," without amplification to the sensitive elements of the recording galvanometer. A potentiometer of high resistance was incorporated in each circuit for balancing the bridge. In order to calibrate the gage installation, access was provided into each circuit by means of jacks so that resistances could be paralleled with the two active arms of the bridge.

In order to establish the blade angular position for peak stress and other trace characteristics relative to propeller angular position, one of the galvanometer elements was utilized as a revolution marker. A special slip-ring and brush combination on the pineapple, which passed current for several degrees only of each complete revolution of the propeller, was connected to this element and a voltage was applied. The resulting trace was a solid line except for a short break occurring once each revolution at the angular position of the propeller corresponding to current passing through the brush and slip ring. This revolution marker defined the propeller angular position to an accuracy of ±2°.

TESTS

A blade setting of 30° at the three-quarter-radius station was employed throughout the tests and constant rotational speeds were used for all tests. Vibratory-stress records were made for one or more tests for each combination of propeller configuration, rotational speed, and pitch angle. Wake-survey data were recorded on all tests.

Tests were first made with the three-blade propeller with the thrust axis coincident with the tunnel axis to establish

a vibratory response arising from factors other than thrust-axis inclination and to obtain wake thrust data on which to base load-vibration predictions. Subsequently, the propeller was tested with its thrust axis inclined to the tunnel axis at angles of 4.55° and 9.80°.

Similar tests with a two-blade propeller were made. Operation of this propeller, however, was restricted to a pitch angle of 4.55° and to rotational speeds not over 2,000 rpm because of anticipated excessive dynamometer vibration.

A limited number of tests were made with a two-blade propeller employing the semiarticulated hub. The hub was designed for one-blade-propeller research and was not properly articulated to alleviate blade stresses most effectively. The tests were conducted to determine whether the propeller disk would orient itself so as to relieve the vibratory stresses due to pitch.

REDUCTION OF DATA

TUNNEL VELOCITY

Airstream velocity was determined by the use of the tunnel calibration normally used for the dynamometer in an untilted condition. While the projected frontal area was increased appreciably by tilting the dynamometer, the cross-sectional-area change at any one position in the tunnel was so small that the effect on the tunnel calibration was negligible. The advance ratios have been corrected for tunnel-wall interference to free-air conditions.

WAKE-SURVEY DATA

In the reduction of wake-survey pressures to section thrust data, the radial and angular locations of each pressure tube of the survey rake were determined for each strut position and pitch angle by assuming that the air flowing through the propeller disk continued parallel to the tunnel axis. Although this assumption is somewhat incorrect over the inboard sections, where the proximity of the inclined spinner undoubtedly affected the air flow, it is believed to represent generally a good approximation to the correct flow pattern. All wake-survey data have been cross-faired in order to obtain data from the several strut positions at identical radial locations and operating conditions. In the determination of incremental thrust-coefficient values, the data used as a zero reference were the thrust coefficients obtained on the untilted propeller.

[STRESS DATA

The strain-gage output as recorded on photographic paper was read directly to obtain vibratory-stress values. The stress was taken as proportional to the trace deflection, the constant of proportionality being determined by calibrations made on each gage installation before and after tests. In some cases, strain-gage records were analyzed in detail to obtain their component frequencies. For such analyses four-diameter enlargements of the desired parts of the records were made. The 12-point Fourier series method was then used to determine the components. In general, only data from the gage located at $x=0.45$ are presented herein because conclusions deduced therefrom are considered representative.

The elements of the recording galvanometer used have a natural frequency of 100 cps and are damped 0.7 of critical value. These characteristics fix the amount of lag of the element in recording the stress variation. For the present

tests, this lag varied from 18° to 30° for first-order vibration. In the case of the element used as a revolution marker, however, no lag is present at the beginning of the short break marking the flow of current because an element at rest begins to move at the same instant that current is applied.

RESULTS AND DISCUSSION

AERODYNAMIC DATA

The results of section-thrust-coefficient measurements for the three-blade propeller at thrust-axis inclination angles of 4.55° and 9.80° are presented in figures 6 and 7. These figures represent a summary of the measured aerodynamic data from these tests and are obtained by conventional fairing procedure from the survey-rake thrust-distribution measurements. For convenience in using the data the curves of C_T' for operation with thrust axis not inclined have been included in all cases.

A few typical examples of section-thrust-coefficient change and of integrated blade-thrust-coefficient change around the disk are presented in figures 8 and 9, respectively. These increments are the differences between values for the tilted and untilted propeller. It is estimated that the fairing of the six points may lead to errors as large as 5° in determining the values of ωt for maximum and minimum thrust coefficient.

Calculated thrust-coefficient change and comparison with measured values.—A consideration of the basic problem of blade excitation, at rotational frequency, caused by inclination of the thrust axis reveals that the fundamental aerodynamic changes may be rather simply described. An analytical method has been devised by which the section aerodynamic-load changes may be computed from two-dimensional airfoil data (ref. 2). If blade-section data for operation of the particular propeller, untilted, are available either from pressure-distribution (lift) measurements on rotating blades or from wake-survey (thrust) measurements, more direct methods may be used in the prediction of the load variations. Regardless of the method used, two fundamental considerations should be borne in mind. First, it must be recognized that the change in blade loading is influenced not only by angle-of-attack changes but also by Mach number changes during a revolution and that the method used to predict the variations must consider both effects. These points are discussed more fully in the appendix. Secondly, a fundamental difficulty likely to be encountered is the lack of sufficient static-airfoil information, so that it becomes necessary to extrapolate the data. Extrapolation is most troublesome at section speeds near the sonic value. The method used in the present report to predict load variations is based on blade-section wake-survey thrust data obtained for this propeller in the unpitched condition and is described in the appendix.

In order to compare calculated data with measured data, section-thrust-coefficient change and integrated blade-thrust-coefficient change have been calculated for the same operating conditions as occurred for the measured data of figures 8 and 9, and the results are presented in these same figures. Some extrapolation of the basic data used for the computations was necessary and has been indicated by the use of broken lines on portions of the calculated curves of figure 8. All of the extrapolation is regarded as conservative with the exception

of parts of a few of the curves at the two most inboard stations. To simplify the comparison, the lag and amplitude of the thrust-coefficient change are considered separately.

Lag of thrust-coefficient change.—Although the aerodynamic lag is not expected to be of importance in the design of an actual propeller blade, interpretation of the results of the present investigation requires that a discussion be included. It is apparent that, if the geometry alone for the pitched propeller is considered, the maximum loading should occur at the 90° position and the minimum loading at the 270° position with the conventions used herein. Since the method used to obtain the calculated values is based on geometric considerations and steady-state data, these peaks occur exactly at the 90° and 270° positions or, in other words, show no lag. The peaks of the measured thrust-coefficient-change curves, however, show varying amounts of lag behind the 90° and 270° points. Table I includes a compilation of these phase differences as obtained for the complete blade from figure 9. It will be noted that, on the average, the minimum peak lags about 16° (column ⑧) and the maximum peak lags somewhat more (column ⑨). Also included in the table are the known causes of phase difference and their estimated amounts. A brief discussion follows.

The oscillatory forces affecting the lag arise from two distinct causes: first, fluctuations of angle of attack in combination with a pulsating air flow, and second, blade flapping. Application of the equations presented in reference 3 to an airfoil oscillating about the 50-percent-chord position reveals that the amount of lag arising from the fluctuation of angle of attack alone can never theoretically be greater than 5.8°, and for the present test conditions the lag was calculated to be 5°. Calculations have been made which consider the combined oscillatory effects of fluctuating angle of attack and flexibility or blade flapping but which assume that the blade is a simple mass concentrated at the 0.7 station and has a single degree of freedom. These assumptions tremendously simplify the problem but undoubtedly reduce the accuracy of the results. It is believed that the phase lags resulting from the combined calculated oscillatory effects (column ④, table I) are in the proper direction but their magnitudes may be inexact.

Because the survey rake was about 10 inches behind the propeller, there is some lag in the measured results due to

twist in the slipstream. This lag was calculated at 0.5° or less for the cases considered here (column ⑤).

Another cause of lag discrepancy is the nonaxial flow of air in the tunnel. A crossflow of about 0.5° and an upflow of considerably less than 0.5° exist through the test section, which leads to a propeller speed excitation not in phase with that due to propeller-axis inclination. Calculations show that the effect will appear in the wake as 3° to 6° of lead rather than lag (column ⑥).

There is a difference between the phase shifts for the maximum and minimum peak measurements (columns ⑧ and ⑨) which may be partially accounted for. As may be noted in figure 8, the difference appears to be caused by the many instances where the value of the section thrust coefficient at the 75° position was markedly low, which so affected the fairing as to cause a greater phase lag at the maximum peak than would otherwise exist. The only tangible explanation appears to be that of interference by the main dynamometer support strut. In the twisting slipstream behind the propeller the strut becomes an airfoil at a small angle of attack, causing a change in the inflow angle locally at the propeller disk. The trend of this effect is in the correct direction but is insufficient to cause more than a small part of the discrepancy.

There still exists an unexplained phase difference of from 7° to 13° between the calculated and experimental angular locations of peak load variation (column ⑫), even for the minimum peak, which is considered to be the more accurately located of the two. Further analysis of blade flapping showed that if more than a single degree of blade freedom were assumed and if an allowance were made for hub flexibility and structural damping, then the difference in the lag between estimated and measured aerodynamic values would be reduced by about 6°. This analysis indicates that the agreement should improve as the assumptions used in the calculations are made more realistic.

Amplitude of thrust variations.—The agreement in magnitude of the computed and measured values of applied-force variation, or change in section thrust coefficient, appears to be good though somewhat erratic at the low rotational speeds (low resultant section velocity). This agreement may be seen in figure 8 in the data for rotational speeds of 1,350 and 1,600 rpm. As the computed values are based

TABLE I

EVALUATION OF PHASE DIFFERENCES

① Propeller speed, rpm	② CT, deg	③ Advance ratio, J	Estimated phase lag, deg				Measured aerodynamic phase lag, deg			⑪ Analyzed 1-P stress lag, deg	Difference, deg, —	
			④ Combined oscillatory effects	⑤ Slipstream twist	⑥ Tunnel crossflow	⑦ Total	⑧ Minimum peak	⑨ Maximum peak	⑩ Average		⑫ Between estimated and minimum peak measured aerodynamic lag, ⑧-⑦	⑬ Between measured aerodynamic average and 1-P stress lag, ⑪-⑩
1,350	4.55	1.20	9.3	0.5	−6.0	3.8	12	20	16	23	8	7
	9.80		9.3	.5	−3.0	6.8	20	22	21	28	13	7
1,600	4.55	1.20	10.6	.5	−6.0	5.1	14	23	19	23	9	4
	9.80		10.6	.5	−3.0	8.1	15	18	17	27	7	10
2,000	4.55	1.25	12.8	.4	−6.0	7.2	18	22	20	19	11	−1
	9.80		12.8	.4	−3.0	10.2	23	28	25	30	12	5
2,160	4.55	1.25	14.0	.4	−6.0	8.4	16	22	19	31	7	12

on simple geometric considerations and steady-state data, it may be concluded that consideration of oscillatory lift forces is unnecessary. At the higher rotational speeds (2,000 and 2,160 rpm) the agreement is not so good. It has proved difficult to ascribe the discrepancy to any particular phenomenon. · A possible explanation for the discrepancy at the higher speeds is that the dynamic lift-curve slope may be appreciably different from the static lift-curve slope for the same average Mach number. In this event the computed values would be in error since they are based on steady-state data.

It seems doubtful, however, that such a difference between the static and dynamic lift-curve slopes would be a predominant factor in the discrepancy. These lift-curve-slope differences would be expected to be dependent on the reduced frequency, which is the flutter parameter commonly used to relate the frequency of oscillation to the blade chord. Throughout these tests the reduced frequency was essentially a constant and, thus, differences between static and dynamic lift-curve slopes, if present, should have been apparent at all rotational speeds.

The calculated values of figure 9 for blade-thrust-coefficient variation show much better agreement with the measured variation than do the section data, especially with regard to the overall or peak-to-peak values. The discrepancies of the section data tend to average out when integrated to obtain blade thrust.

To show further the agreement in magnitude between computed and measured values of blade thrust variation, one-half of the peak-to-peak displacements of the thrust-coefficient-variation curves shown in figure 9 have been converted to pounds of thrust and plotted in figure 10. The close agreement is apparent. For the abscissa in this figure, the product of the pitch angle and the free-stream dynamic pressure $\alpha_T q$ has been used, since it may be shown that the exciting force theoretically varies directly with this product. The linearity is illustrated by the straight line drawn from the origin. A derivation of the parameter $\alpha_T q$ may be found in reference 4.

It might be thought that the severe effects of compressibility encountered at the higher rotational speeds would destroy the linearity in figure 10. However, the compressibility effects, while severe, result in a shift of the loading toward the inboard sections and do not seriously affect total blade thrust variation as shown in figure 10. The reapportionment of the load between the inboard and outboard sections is illustrated in figure 11, where one-half of the measured peak-to-peak section-thrust-coefficient change for each blade station is plotted against blade radius for four rotational speeds at the same inclination angle.

STRESS DATA

Data from the strain gage located at the $x=0.45$ station were selected for detailed analysis because it was the approximate location of maximum blade stress and because data obtained therefrom were considered to be representative. It should be recognized that the stresses measured by the gage located at $x=0.45$ represent the effect of vibratory forces on all of the blade outboard of $x=0.45$ and not on that station alone.

An inspection of the vibratory stress records obtained in the current tests indicated the presence of excitations at frequencies other than the principal propeller-speed excitation frequency. It was necessary, therefore, to perform a harmonic analysis of the vibration records to isolate the once-per-revolution, or 1-P, vibration component. The assumption that the resulting first-order stress curve is a true representation of the stress variation due to inclination of the thrust axis cannot be fully justified because the harmonic analysis performed results in a first-order stress variation which is a true sinusoid, whereas the expressions derived for the thrust-coefficient variation (see appendix) indicate that this excitation is not exactly sinusoidal.

The extraneous orders of stress excitation were largely twice-per-revolution, or 2-P, which, at the lowest rotational speeds, closely approached resonance. Higher-order frequencies were noted but were generally small in magnitude.

. **Lag values.**—In order to obtain stress-lag data which could be compared with the lag values from figure 9 as given in table I (column ⑩), the galvanometer traces analyzed were from test points for which the operating conditions duplicated as closely as possible those of figure 9. The lag values thus obtained from the 1-P component of the trace, corrected for galvanometer-element lag, are included in table I (column ⑪).

The phase shift between the impressed force (measured aerodynamic average) and the analyzed 1-P trace maximums is from −1° to 12° (column ⑬) and averages about 6°. The agreement is considered reasonable because of the accuracy of interpretation of timing (±2°) and of aerodynamic phase shift (±5°).

Magnitude of stresses.—It was desired to investigate the trend in measured stresses by using the same parameter $\alpha_T q$ as was used for the exciting force in figure 10. The test conditions chosen to obtain the points for this plot (fig. 12 (a)) approximate peak propeller efficiency conditions but do not duplicate those for the thrust comparison plot of figure 10. For some combinations of rotational speed and thrust-axis inclination, data from two points near peak efficiency were analyzed so as to indicate the shift in stress with a slight change in advance ratio. The stress points at the low rotational speeds conform to a linear relationship; however, the stresses obtained for the higher rotational speeds (2,000 and 2,160 rpm) are lower than would be indicated by a linear extension of the low-speed values. The lower stress values at the higher rotational speeds were to be expected because figure 11 indicated an inboard movement of the change in load with increased rotational speed, and the stresses at the blade station considered would thus be reduced below that anticipated by a linear extrapolation. This fortunate attenuation of the stresses when the outer portions of the blade are in the transonic and low-supersonic speed range will lead, therefore, to a conservative design if the design is based on the conditions existing at the lower rotational speeds. When all sections are operating supersonically, this stress attenuation will become less because the blade loading will revert to a loading similar to that found in the subsonic case.

In order to establish that this stress reduction is associated with the inboard movement of load with increased rotational

speed, a blade vibratory stress calculation based on both measured and predicted aerodynamic-load variations was made for each of the experimental values of figure 12 (a). The method of calculation involved finding by an iterative process the correct moment distribution along the blade. At the two lower rotational speeds, both measured and calculated thrust-change data have been used to compute blade stresses; however, at the two higher rotational speeds the stress values have been determined only from measured values of section-thrust-loading change because of the excessive extrapolation required to obtain calculated thrust-loading change.

The stress values determined by the calculations are plotted in figure 12 (a) and indicate considerably lower stresses than were measured because the magnification of the stresses associated with an approach to resonance has not been accounted for. The natural frequency at each rotational speed was then calculated from the usual equation

$$f^2 = f_0^2 + cn^2$$

by using an assumed centrifugal-correction factor c of 1.7 for the first mode and a static natural frequency determined by bench tests to be 28.8 cps. The magnification factor at each rotational speed was determined, at the proper ratio of propeller speed frequency (1-P) to natural frequency, from the conventional response curve for forced vibration of a system with a single degree of freedom and approximately zero damping. The computed stresses when corrected by this amplification factor are also lower than the measured stresses (fig. 12 (b)). However, reduction in the magnitude of blade thrust variation caused by the inboard movement of the load is verified by the reduction in stress at a rotational speed of 2,160 rpm.

So far only peak propeller efficiency conditions have been considered. The parameter $\alpha_T q$ must be modified in any comparison of stresses for widely divergent operating conditions. The parameter should take into account the actual lift coefficient, geometric helix angle, and lift-curve slope. The full expression for the maximum amplitude of the periodic lift on a small length of blade Δr has been derived in reference 4 and, in the notation of the present report, is:

$$\alpha_T q (a + 2c_l \cot \phi_0) b \ \Delta r$$

The factor $\alpha_T q$ was therefore multiplied by $(a + 2c_l \cot \phi_0) b$ to obtain the modified form, the theoretical lift-curve slope corrected for Mach number being used rather than the undetermined actual slope. The stresses plotted in figure 13 against the resulting modified $\alpha_T q$ were obtained from unanalyzed data, but the error introduced by the omission of a harmonic analysis was investigated and found not to affect the comparison of the resulting curves. The net effect of the modification of $\alpha_T q$ is to give a linearity to all of the stress data at the low rotational speeds. The comparison indicates

the same trend, however, as for the peak efficiency points plotted in figure 12. It should be noted that this comparison is largely dependent on the choice of a representative blade station, $x = 0.7$ in the present case; however, at no station was the expected linearity of the relation between stress and $\alpha_T q$ achieved for all speeds. The conclusions may therefore be drawn that lift coefficients and lift-curve slopes at high section Mach numbers are not given full consideration in the method of application.

Comparison of stresses for two-blade and three-blade propellers.—A comparison is made, in the following table, of blade stresses at $x = 0.5$ for the three configurations investigated (three blades, two blades in rigid hub, and two blades in semiarticulated hub) at several rotational speeds:

Propeller rotational speed, rpm	Vibratory stress at $x=0.5$, lb/sq in.		
	3-blade	2-blade	2-blade semi-articulated
1,350	±794	±840	±528
1,600	±1,008	±1,100	±460
2,000	±1,203	±1,256	----------

The stress values were all obtained at a propeller-thrust-axis inclination of 4.55° and are for values of J which represent the advance ratio for peak efficiency of the three-blade propeller.

The table compares maximum vibratory stresses without regard to the orders of propeller vibration present because the original stress records showed varying percentages of 1-P stress. The stresses for the three-blade propeller were predominantly 1-P and were of the same order of magnitude as those for the two-blade rigid propeller, which, however, contained somewhat more of the 2-P component. The semiarticulated two-blade propeller indicated stresses considerably reduced from those for a rigid propeller. The reduction indicates a reorientation of the propeller plane in such a manner as to reduce greatly the first-order stresses but is accompanied by an increase in higher order stresses, principally 2-P. At least a part of this 2-P vibration was probably caused by the type of articulation incorporated in the hub. With this type of articulation, an oscillatory component is superimposed on the steady component of rotational speed which is transmitted to the propeller. This oscillation is of twice-per-revolution frequency and will be present whenever the propeller plane is not normal to the shaft.

CONCLUSIONS

The following conclusions may be drawn from the present tests:

1. The aerodynamic exciting force that results from a pitched attitude of the propeller may be calculated with adequate accuracy at low rotational speeds.

2. The accuracy of the calculated values of section aerodynamic exciting force when section speeds approach the sonic value is not always as satisfactory as at the low rotational speeds.

3. In the prediction of aerodynamic-load changes of a propeller inclined to the airstream, it is desirable to use section data in a manner that allows for the change of characteristics with change of Mach number around the disk. Such a procedure becomes necessary when sections operate at transonic speeds.

4. The first-order vibratory stress was proportional to the product of thrust-axis inclination and dynamic pressure at low rotational speeds. The stresses at the high rotational speeds were lower than would be anticipated if the stresses were estimated by extrapolation of the low-rotational-speed stresses.

Langley Aeronautical Laboratory,
   National Advisory Committee for Aeronautics,
      Langley Air Force Base, Va., *April 20, 1950.*

APPENDIX

A METHOD OF CALCULATING AIR-LOAD VARIATIONS ON A TILTED PROPELLER

GENERAL DESCRIPTION OF METHOD

A consideration of the geometry of a propeller operating with its thrust axis inclined to the airstream permits determination of the instantaneous values of J and other variables that fix conditions on the blade. If the values thus obtained are applied to the known loading-characteristic curves of the same propeller for the untilted condition, it is possible to predict the instantaneous loading on the blade at any desired point in the cycle of load variation which takes place in each complete revolution. This procedure neglects the dynamic effects of a changing angle of attack and a pulsating air velocity on airfoil characteristics but, since the wavelength of these variations will be a number of chord lengths, the effects should be small. Also neglected are the inertia effects of the changing physical distortion of the blade which will be associated with forced vibration of the propeller.

VELOCITY DIAGRAMS

A velocity diagram showing the three-dimensional character of the velocity variation affecting the blade section is shown in figure 14 (a). Induced velocities have been neglected. Relative to the blade section, the airstream velocity vector V moves so as to cause the resultant velocity vector W to vary not only in magnitude but also in direction. The directional variation effects a cyclic change in both the angle of attack and the sweep angle.

If all velocity components parallel to the blade axis are neglected, that is, those components that cause the sweep-angle variation, a simplified diagram may be drawn, as in figure 14 (b). In order to retain the customary convention which requires an airstream velocity vector at right angles to the rotational velocity vector, the blade section is considered to be operating with an airstream component of $V \cos \alpha_T$ constant in direction and magnitude and with a rotational component $\pi n D x + V \sin \alpha_T \sin \omega t$ constant in direction but varying in magnitude as the propeller rotates.

The apparent instantaneous value of the rotational speed $n_{\omega t}$ can then be determined:

$$\pi n_{\omega t} D x = \pi n D x + V \sin \alpha_T \sin \omega t$$

$$n_{\omega t} = n + \frac{V \sin \alpha_T \sin \omega t}{\pi D x}$$

The instantaneous value of the advance ratio $J_{\omega t}$ will be

$$J_{\omega t} = \frac{\pi x \cos \alpha_T}{\dfrac{\pi x}{J} + \sin \alpha_T \sin \omega t}$$

The diagram of figure 14 (b) and the value of $J_{\omega t}$ derived therefrom are identical with those of reference 2.

CONSTRUCTION OF PLOTS FOR DETERMINATION OF INSTANTANEOUS VALUES OF C_T'

It is now necessary to convert the section thrust data for the untilted propeller into a form suitable for the determination of the instantaneous values. Such a form is represented by the plots of figure 15, in which the section thrust-coefficient values for several values of rotational speed are plotted for the untilted propeller and the curves of constant J are cross-faired on the plots. In this form, the instantaneous value of section thrust coefficient $C_T'{}_{\omega t}$ at any desired condition within the scope of the plot and for any angular position of the blade may be read directly when the forward-velocity component $V \cos \alpha_T$ and the instantaneous advance ratio $J_{\omega t}$ are known.

The value of $C_T'{}_{\omega t}$ thus read, however, is based on an apparently varying rotational speed $n_{\omega t}$ and must be corrected to the true rotational speed n. The conversion is readily made (ref. 2):

$$C_T'{}_{\omega t (corr)} = C_T'{}_{\omega t} \left(\frac{n_{\omega t}}{n}\right)^2$$

$$= C_T'{}_{\omega t} \left(1 + \frac{J}{\pi x} \sin \alpha_T \sin \omega t\right)^2$$

Attention should be called to the effects of supercritical section velocities on the air-load variations obtained by tilting the propeller. As shown on the plots of figure 15, the thrust coefficient for constant advance ratio drops rather sharply as the rotational speed is increased beyond 2,000 rpm for sections outboard of the $x=0.7$ station. This drop corresponds to the reduction of lift coefficient for constant angle of attack experienced with most airfoils as the speed is increased beyond the force-break Mach number. The effect on the section thrust-coefficient variation and thus on the resulting vibration is that of relief, in that the variation experienced is greatly lessened over that which would have been expected had the drop not occurred. It is therefore important that the variation of lift coefficient with Mach number be considered as well as the lift-curve slope. There are probably several methods other than the one presented herein by which these effects can be included. It is important, however, that both variables be accounted for. The results obtained by a consideration of the lift-curve slope alone will be satisfactory for the lower section speeds where the change of lift coefficient with Mach number is small. In the region where the value of the lift coefficient is changing rapidly with Mach number, the predictions will be considerably in error.

REFERENCES

1. Rogallo, Vernon L., Roberts, John C., and Oldaker, Merritt R.: Vibratory Stresses in Propellers Operating in the Flow Field of a Wing-Nacelle-Fuselage Combination. NACA TN 2308, 1951.
2. Crigler, John L., and Gilman, Jean, Jr.: Calculation of Aerodynamic Forces on a Propeller in Pitch or Yaw. NACA TN 2585, 1952. (Supersedes NACA RM L8K26.)
3. Silverstein, Abe, and Joyner, Upshur T.: Experimental Verification of the Theory of Oscillating Airfoils. NACA Rep. 673, 1939.
4. Stulen, F. B.: The 1xP Propeller Vibration Problem and Related Effects. Rep. No. C–2131, Curtiss-Wright Corp., Propeller Div. (Caldwell, N. J.), Jan. 18, 1950.
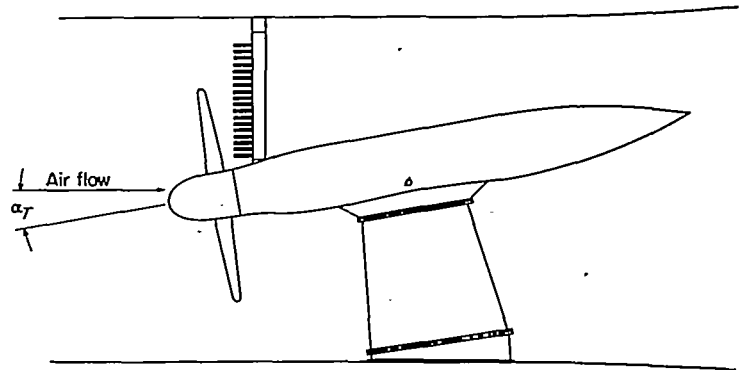
FIGURE 1.—Dynamometer and survey strut.
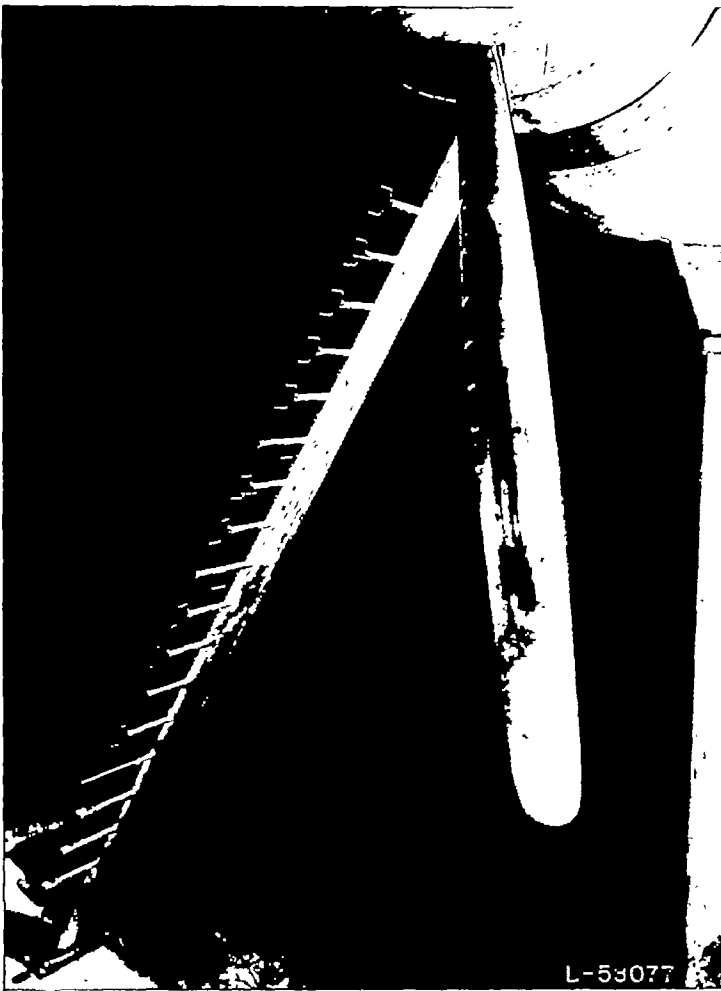
FIGURE 2.—Closeup of survey rake.
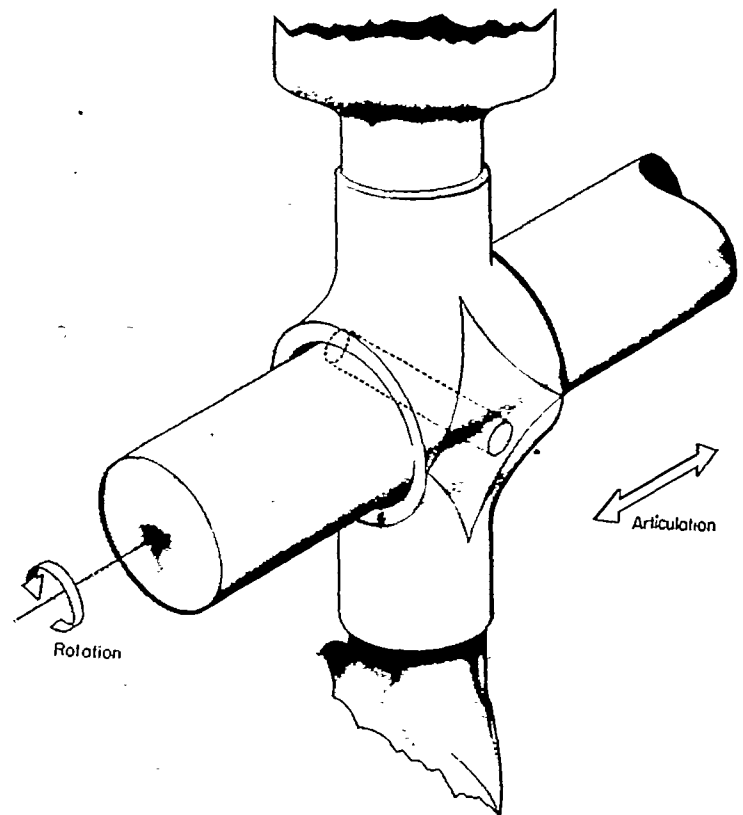
FIGURE 4.—Schematism of semiarticulated propeller hub.
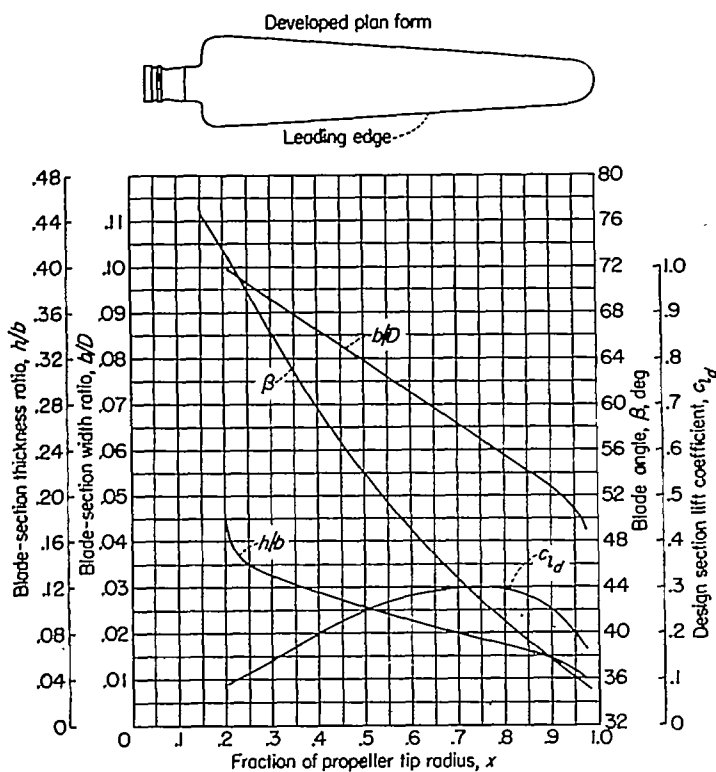
FIGURE 3.—Blade-form curves for NACA 10–(3)(08)–03 propeller.

A,B   Active-arm gages
C,D   Dummy-arm gages
F   Calibration terminals
G   Recording galvanometer
H   Balance potentiometer
J   Galvanometer damping
R_1,R_2 Calibration resistors
S   Slip rings
V   Voltage across gages
(Identical arrangement for additional gages)
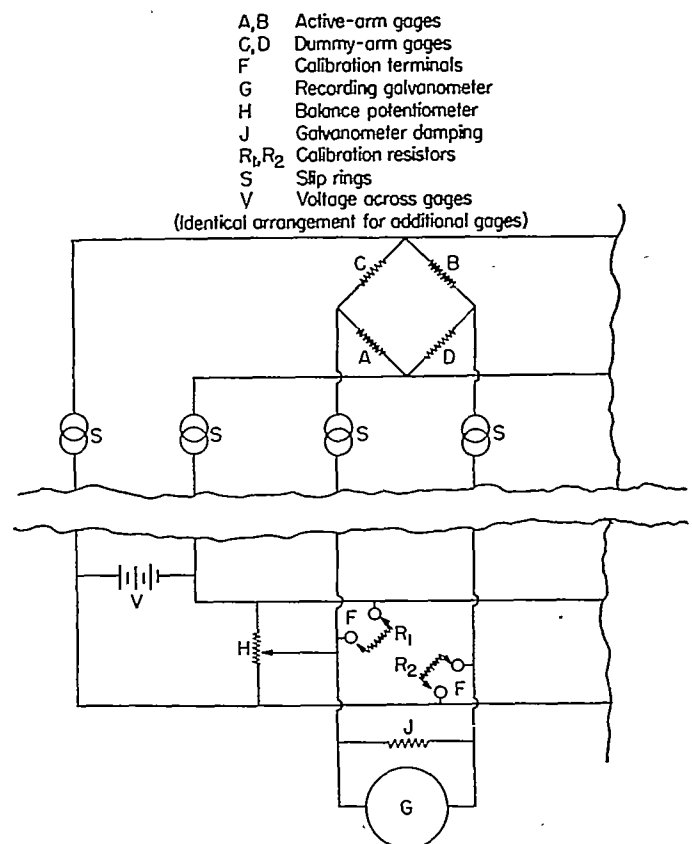
FIGURE 5.—Wiring diagram.

(a) $x=0.3.0$
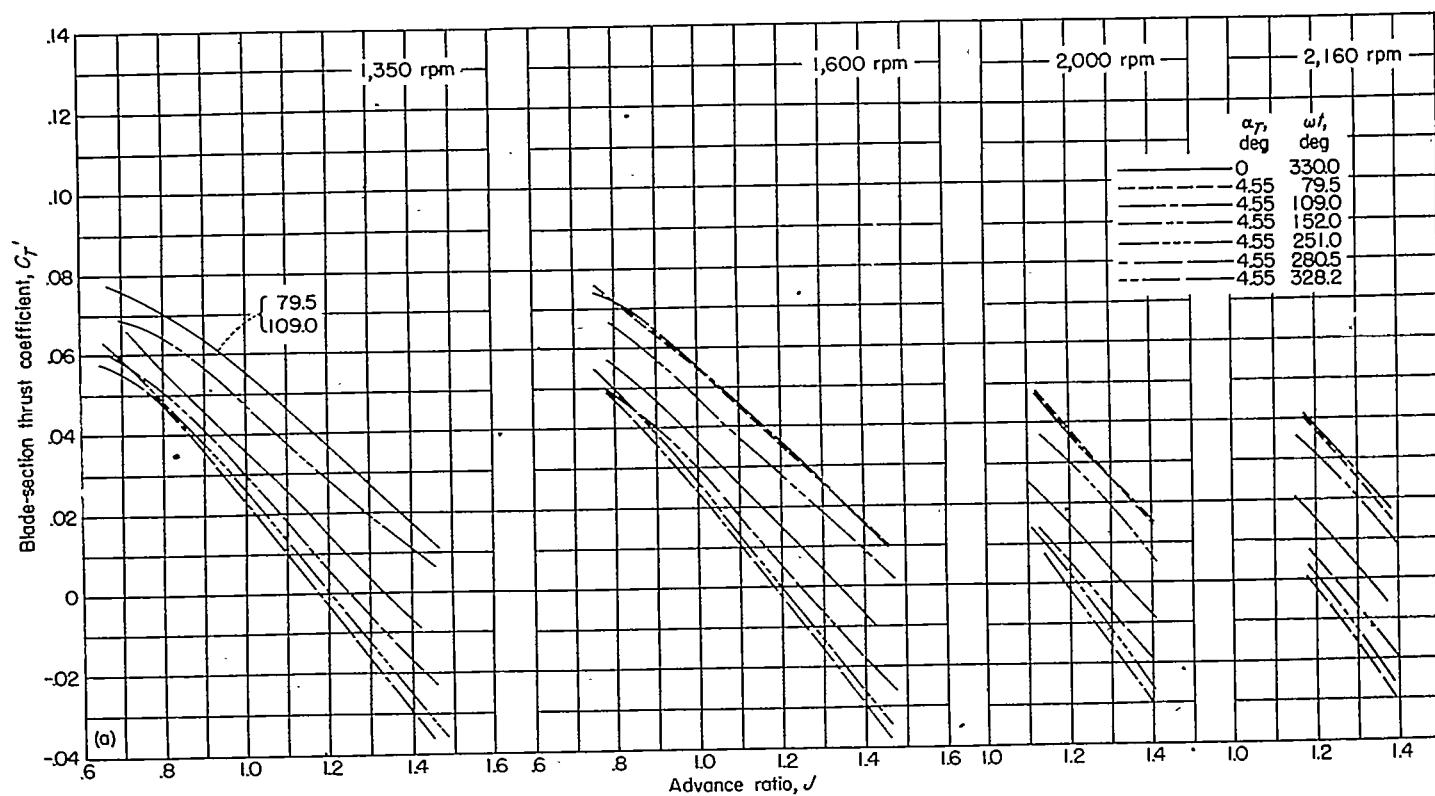
FIGURE 6.—Section thrust coefficient for three-blade propeller. $\alpha_T=4.55°$.

(b) $x=0.45$.
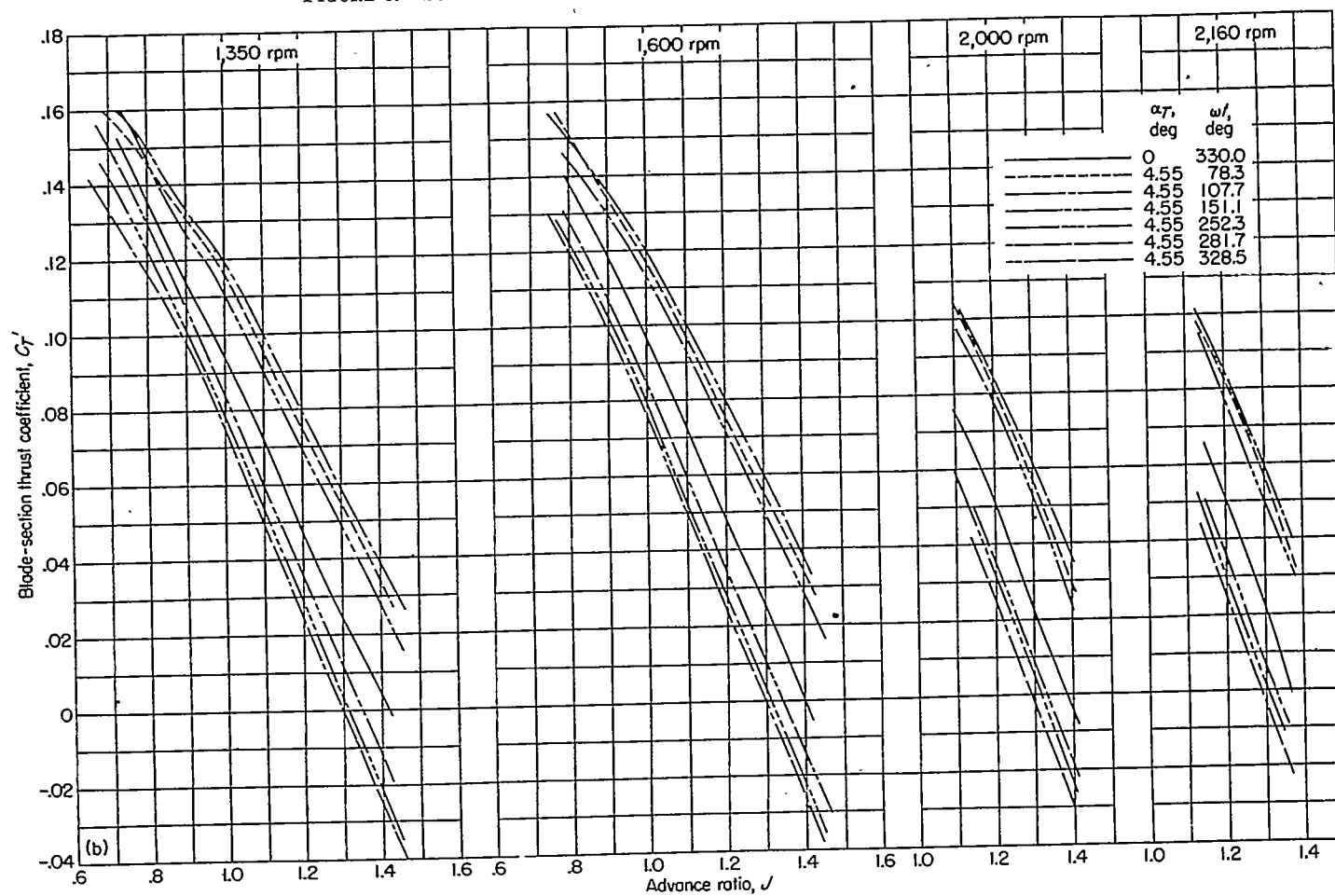
FIGURE 6.—Continued.
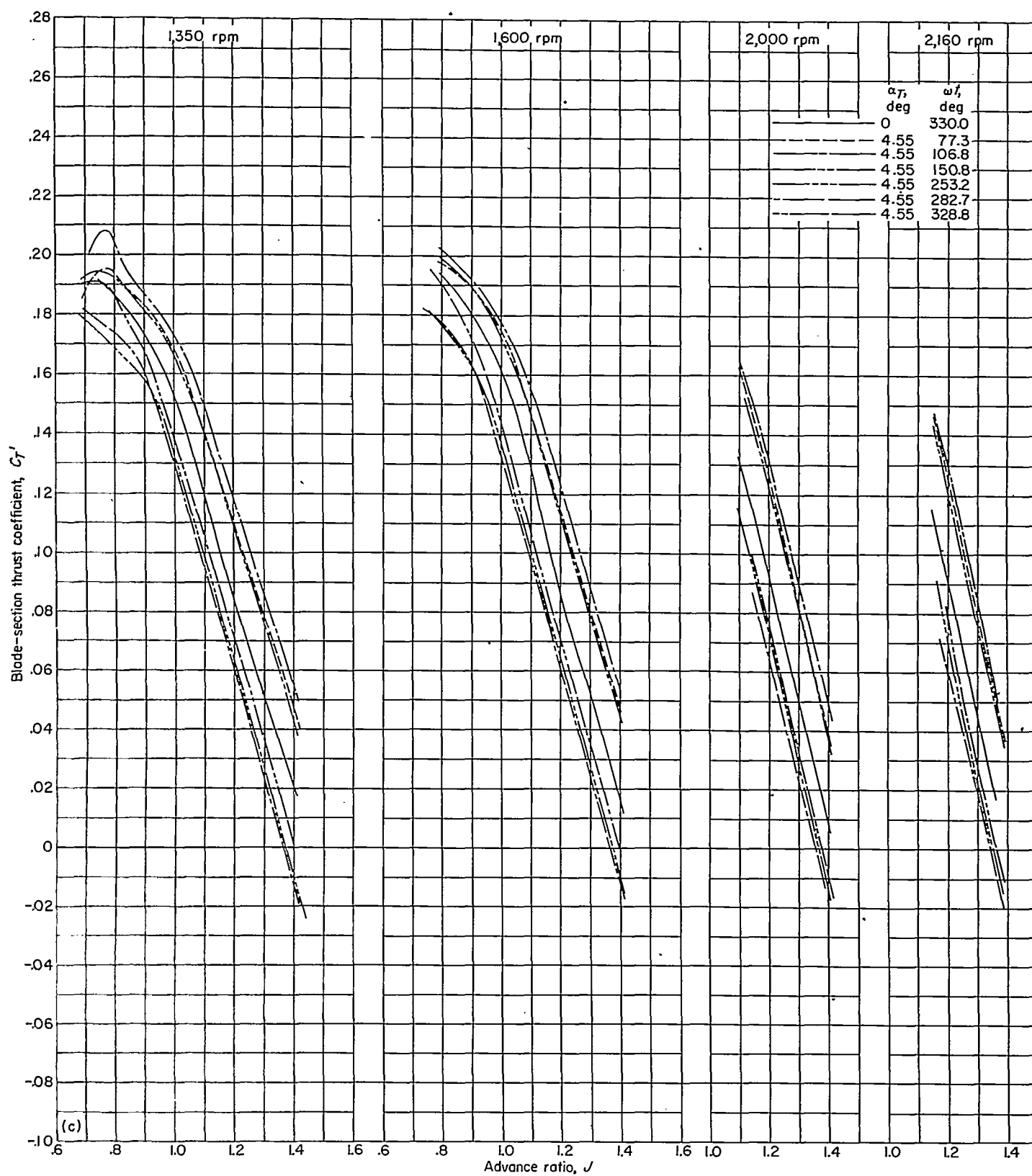
(c) $x=0.60$.

FIGURE 6.—Continued.
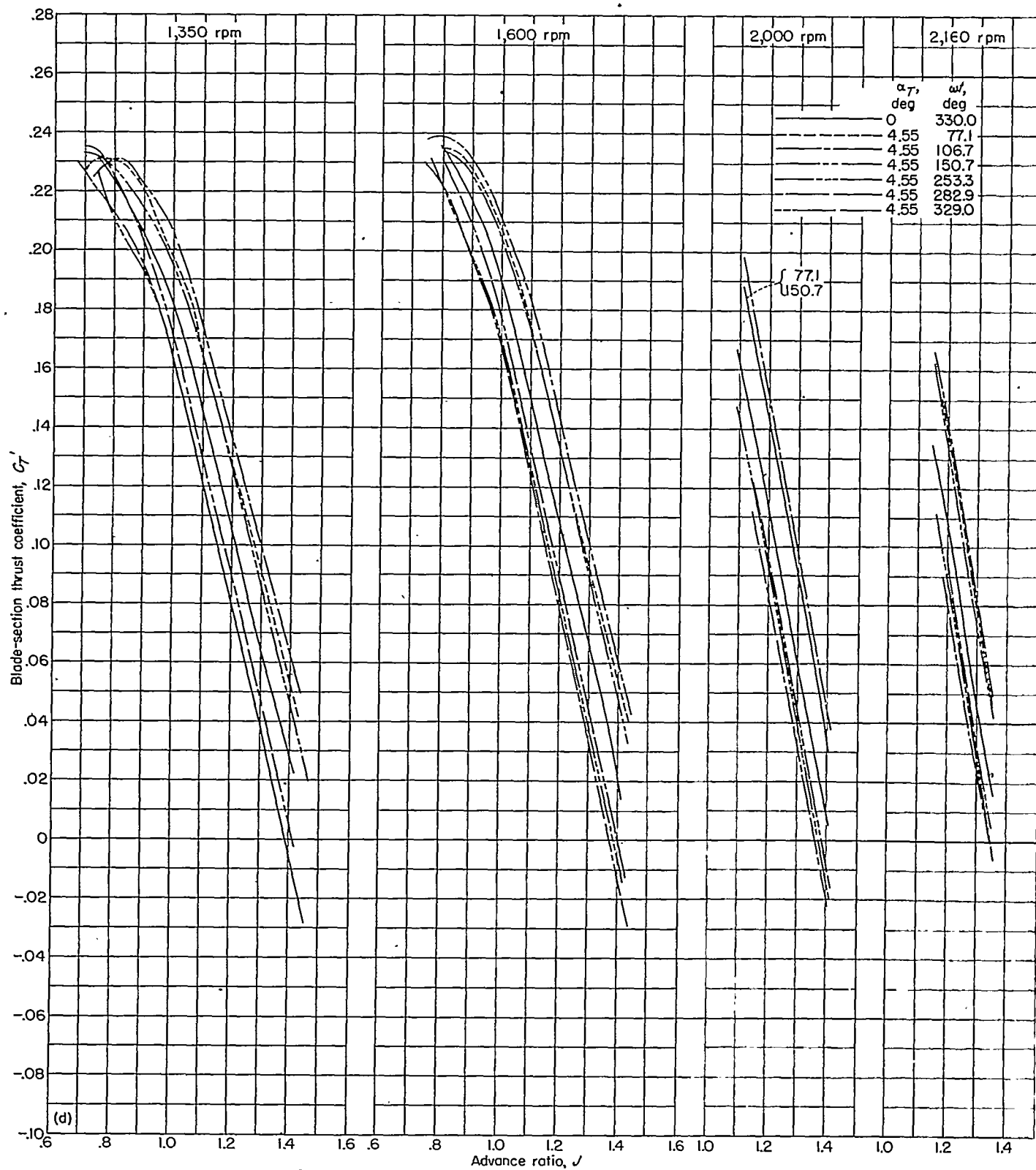
(d) $x=0.70$.

FIGURE 6.—Continued.
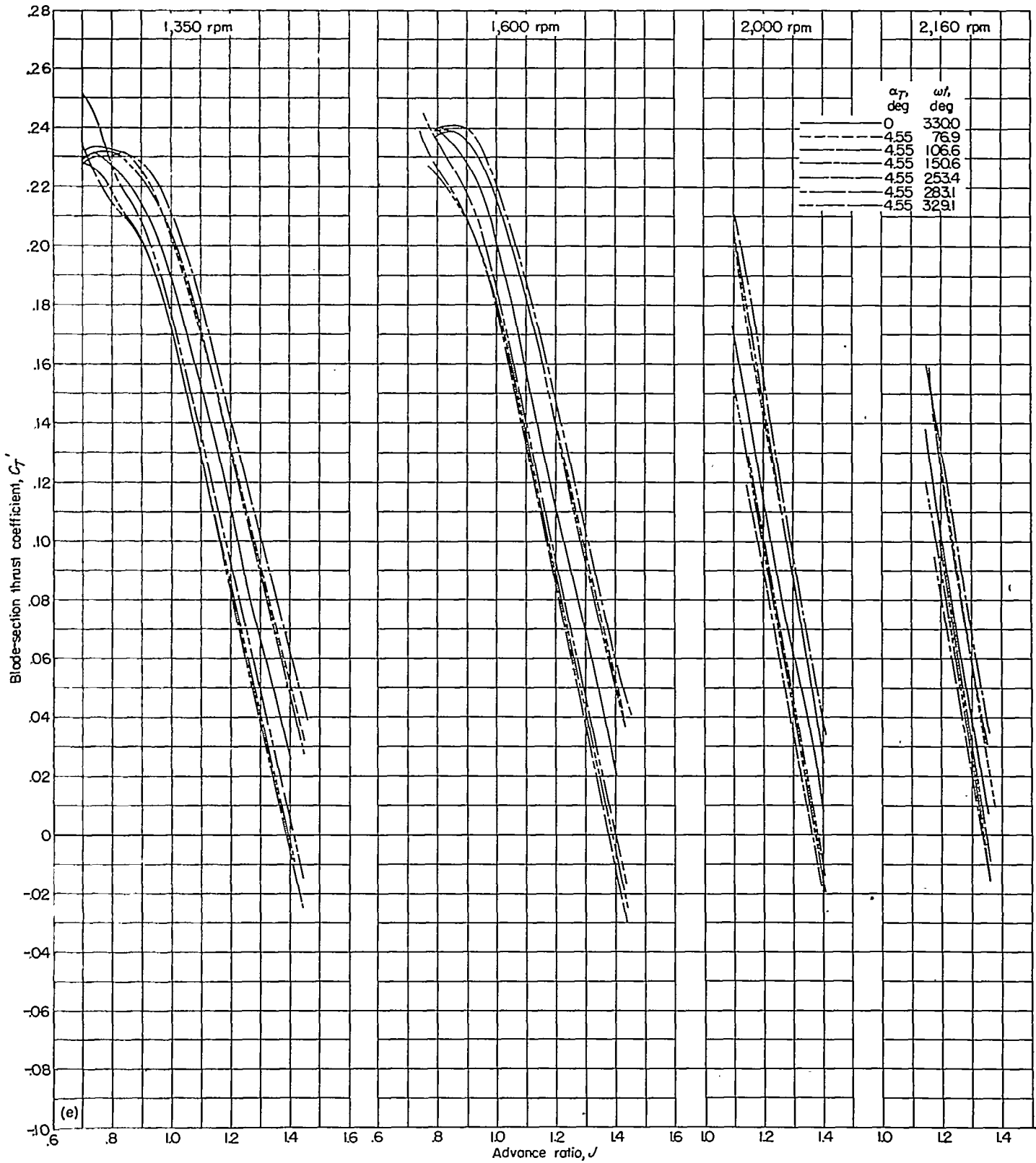
(e) $x=0.75$.

FIGURE 6.—Continued.

(f) $x=0.80$.
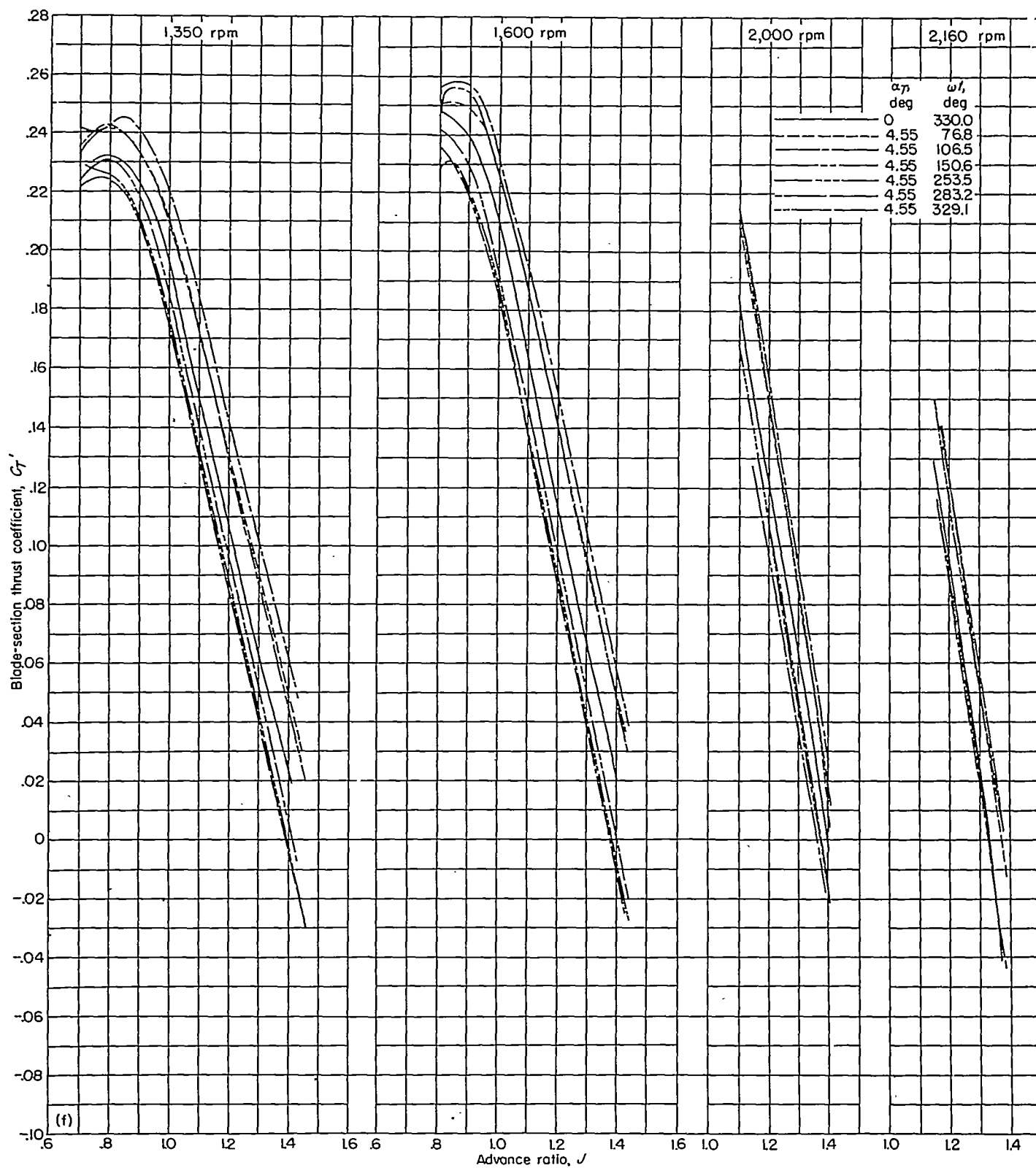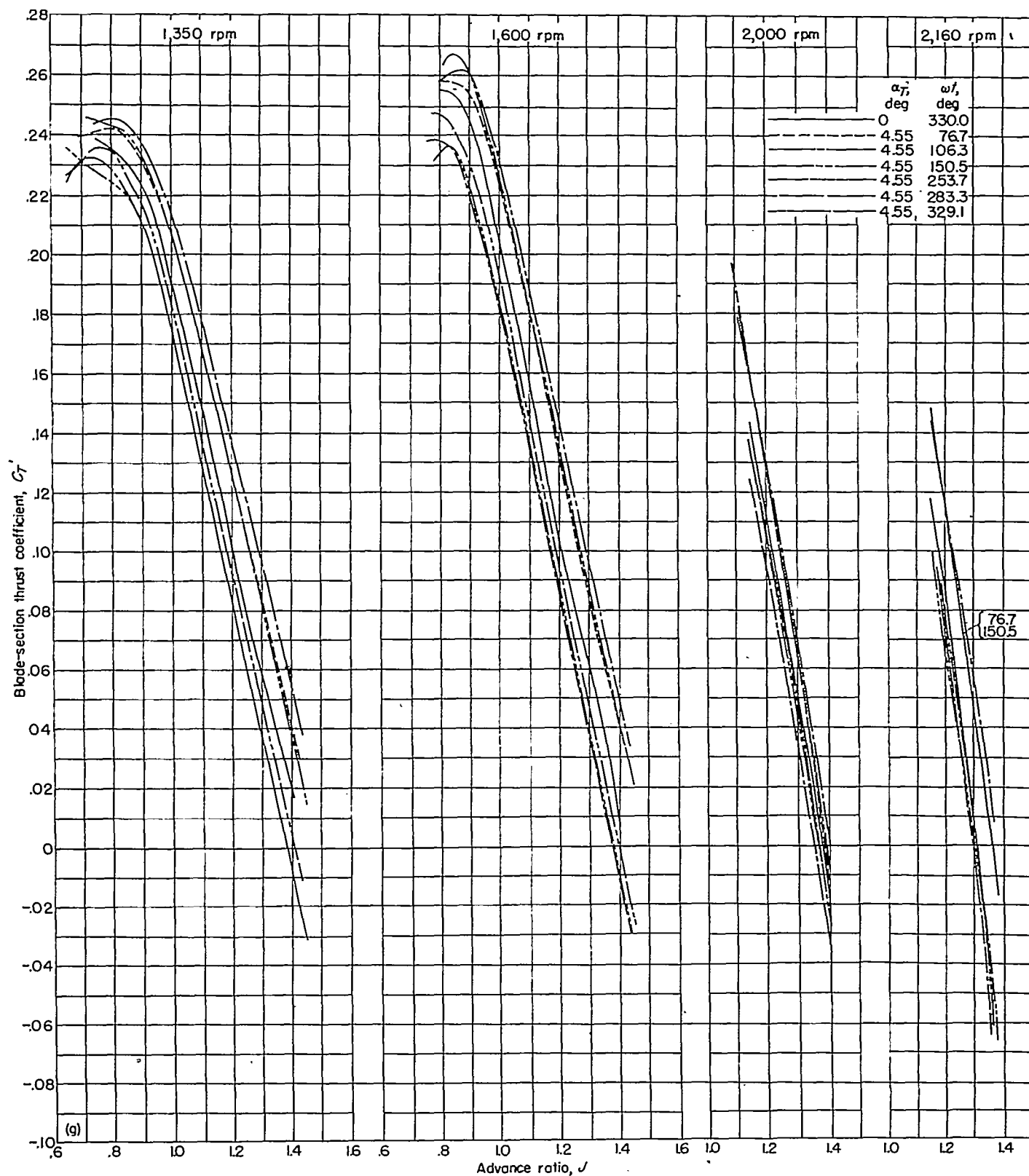
FIGURE 6.—Continued

(g) $x=0.85$.

FIGURE 6.—Continued.
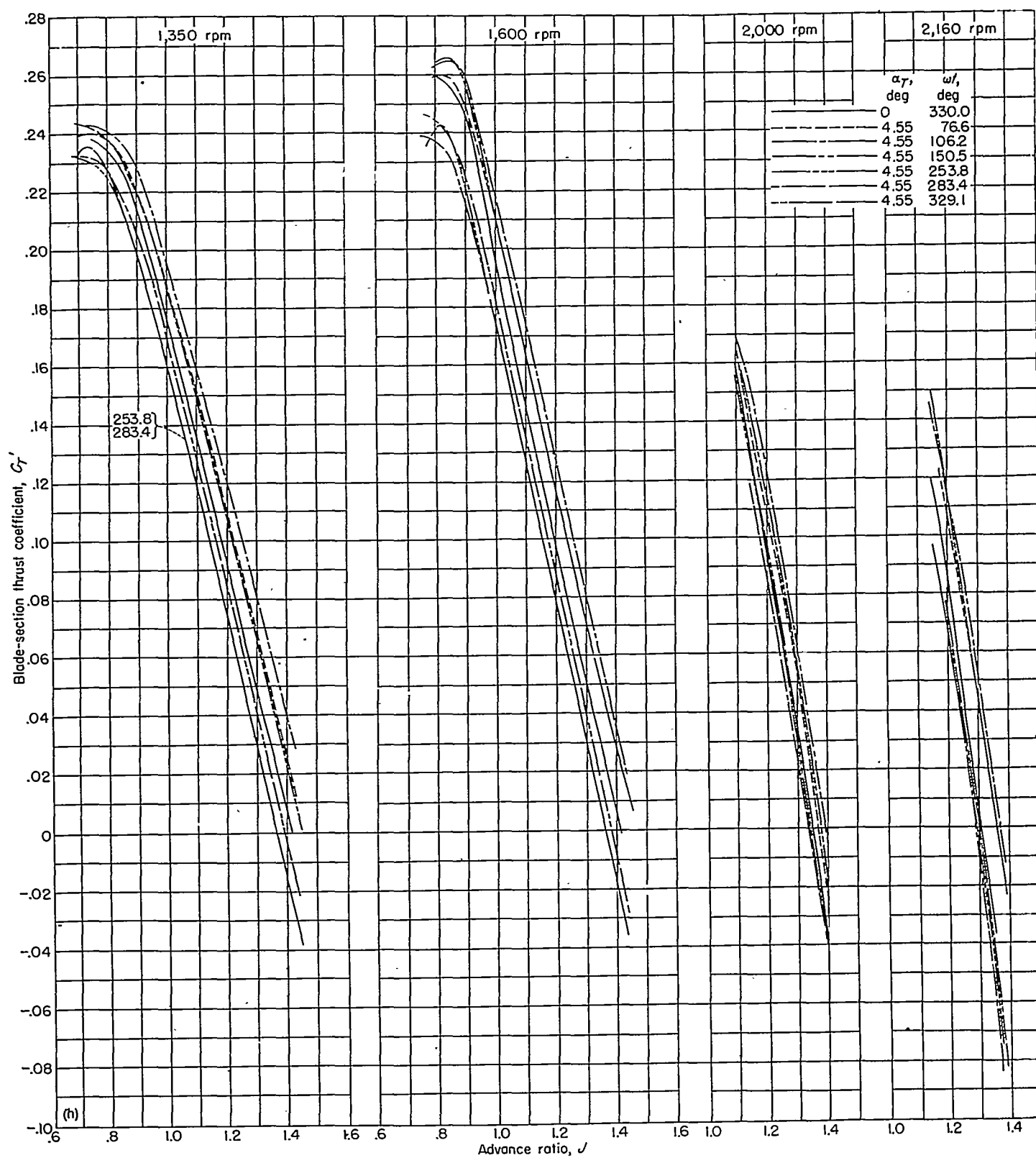
(h) $x=0.90$.

FIGURE 6.—Continued.

(i) $x=0.95$.
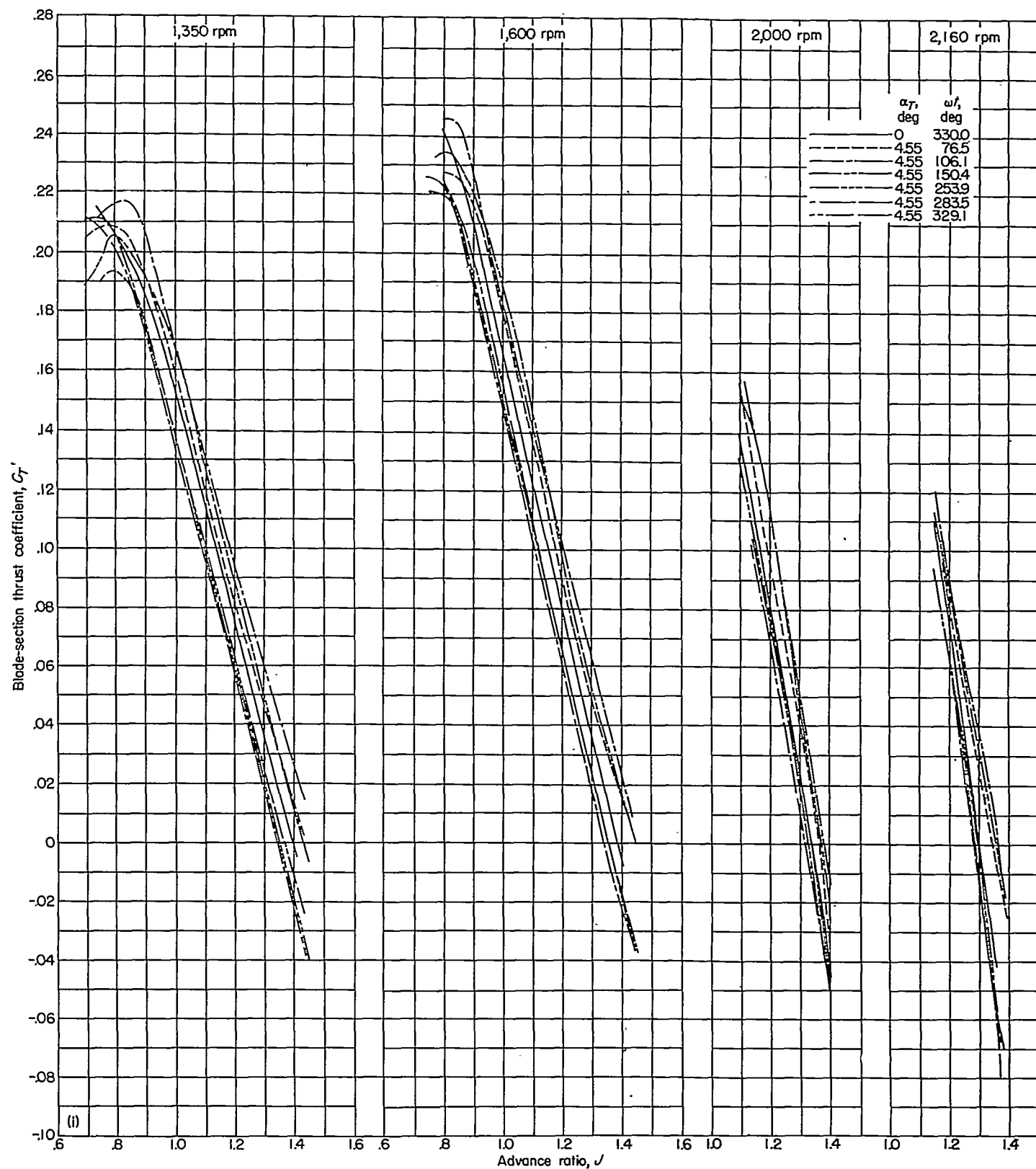
FIGURE 6.—Concluded.

(a) $x=0.30$.
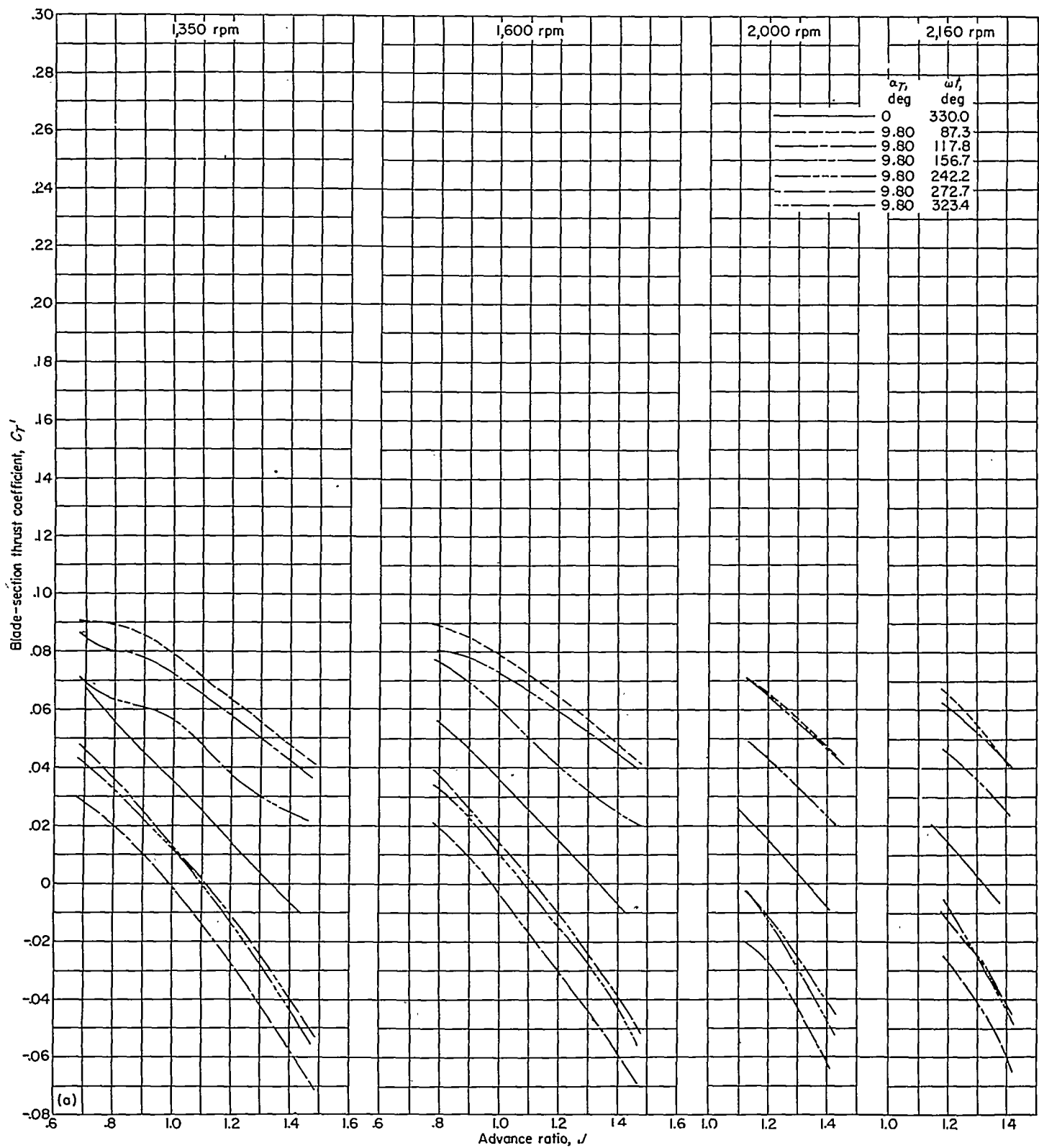
FIGURE 7.—Section thrust coefficient for three-blade propeller. $\alpha_T=9.80°$.

α_T, deg	ωl, deg
0	330.0
9.80	83.3
9.80	113.4
9.80	154.6
9.80	246.6
9.80	276.7
9.80	325.4
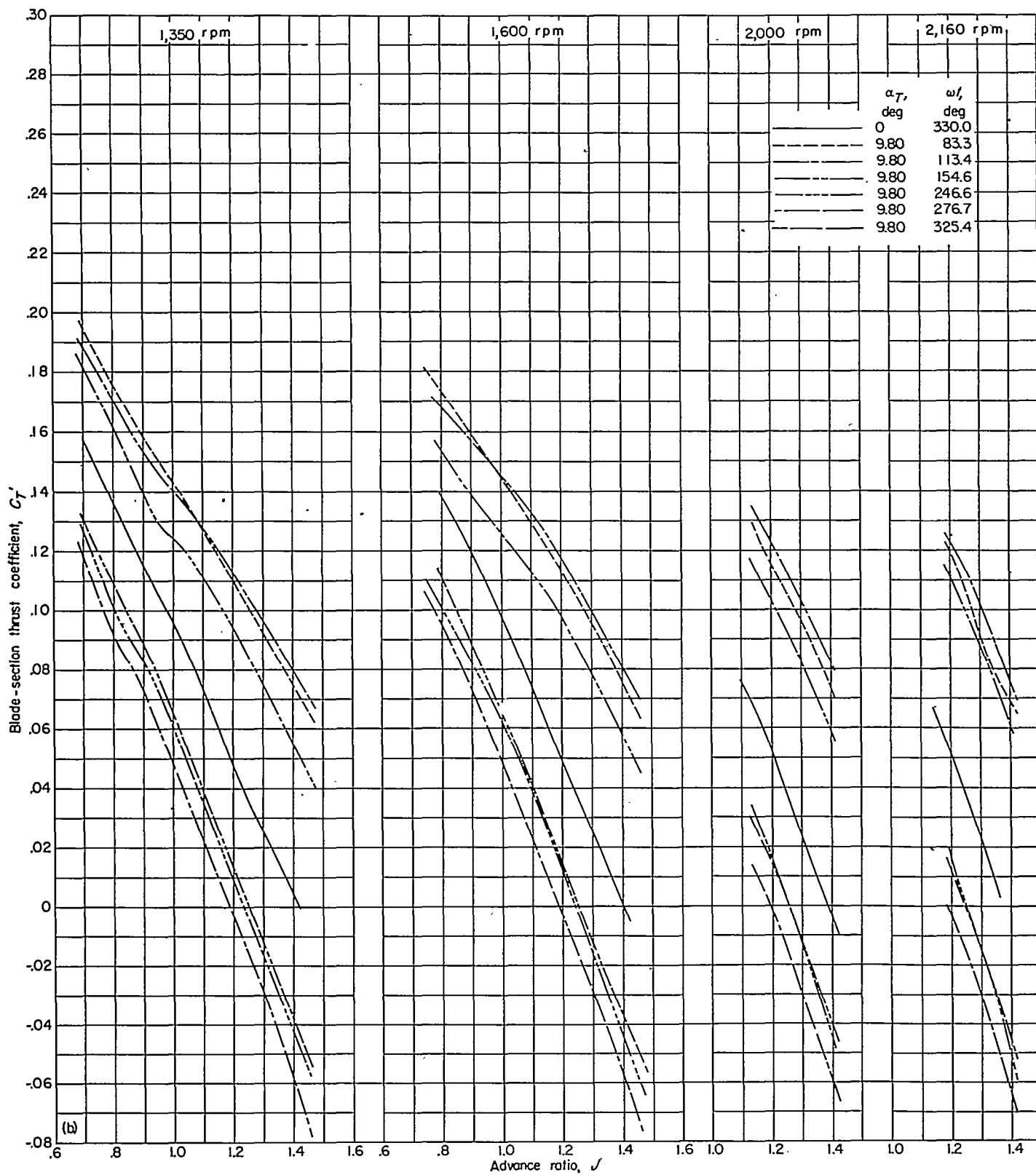
(b) $x=0.45$.
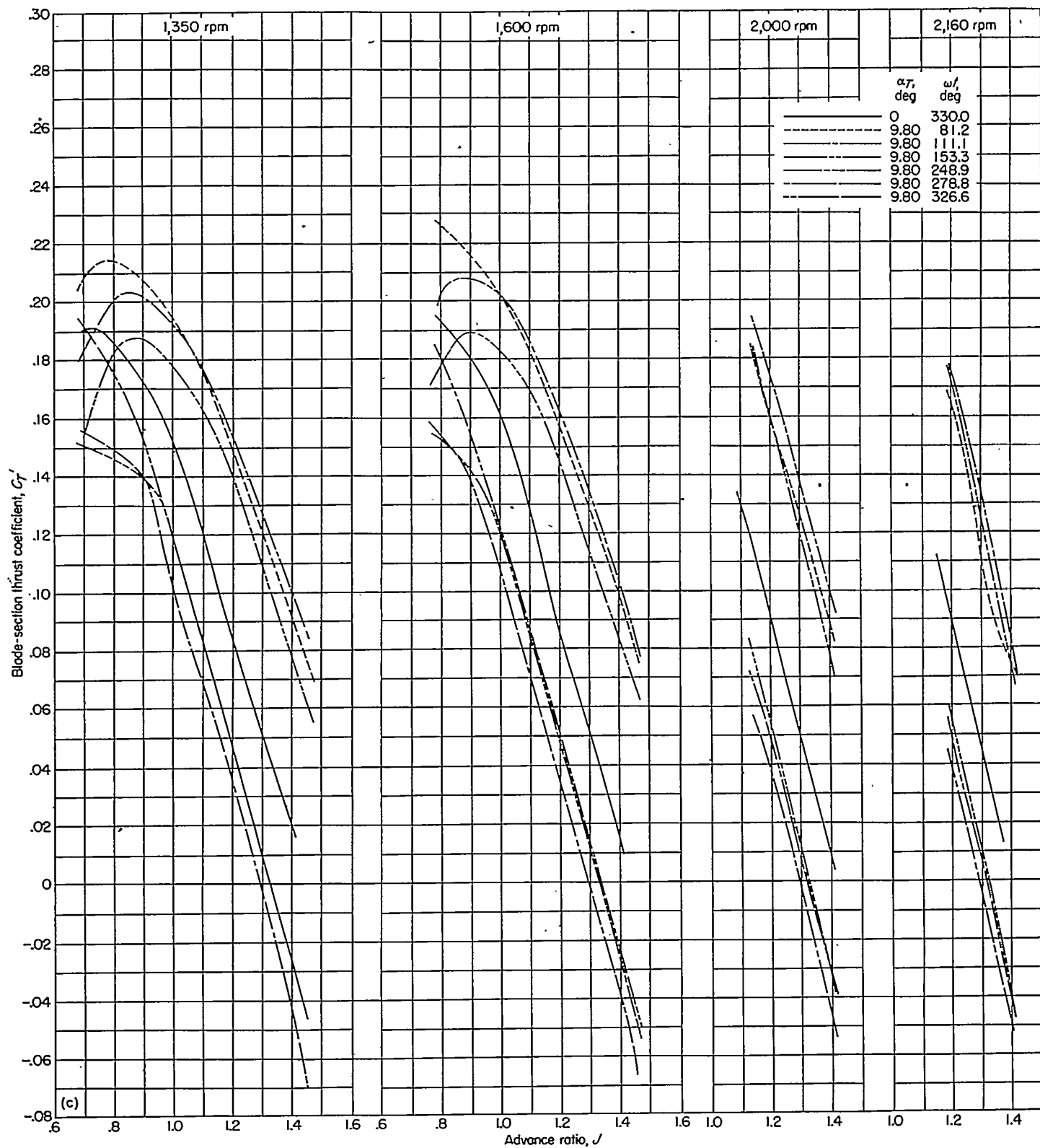
FIGURE 7.—Continued.

(c) $x = 0.60$.

FIGURE 7.—Continued.
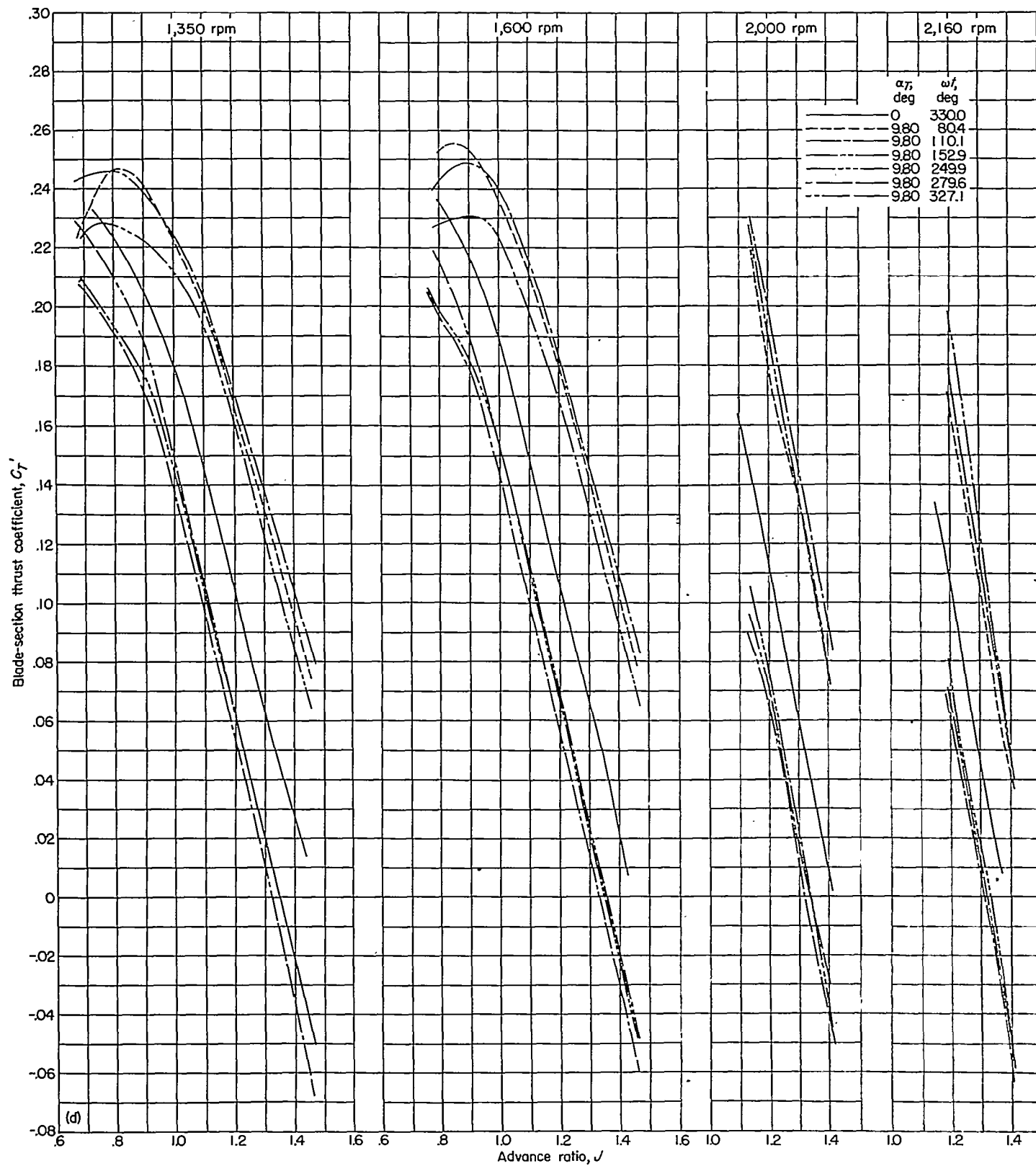
(d) $x=0.70$.

FIGURE 7.—Continued.
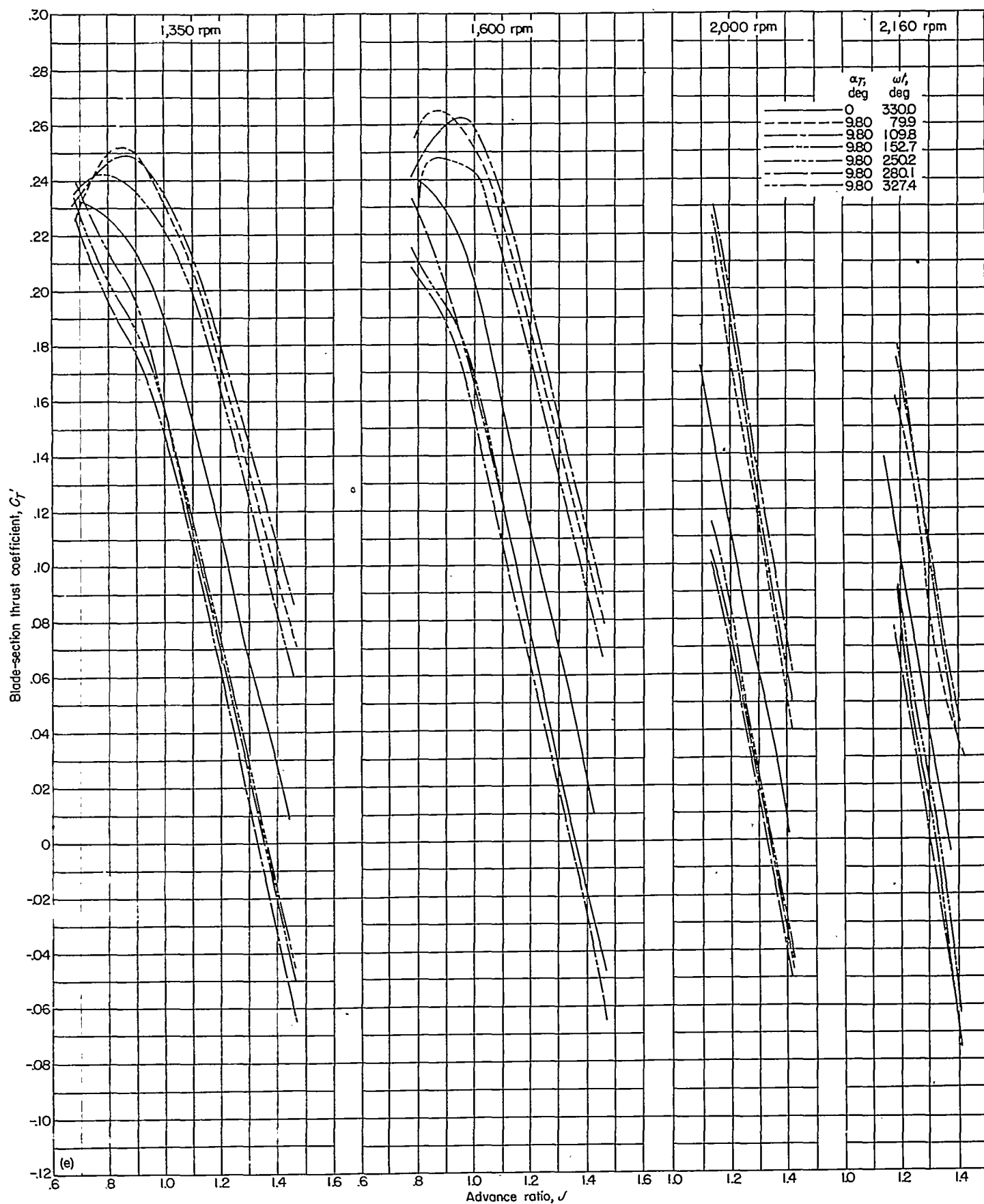
(e) $x=0.75$.

Figure 7.—Continued.
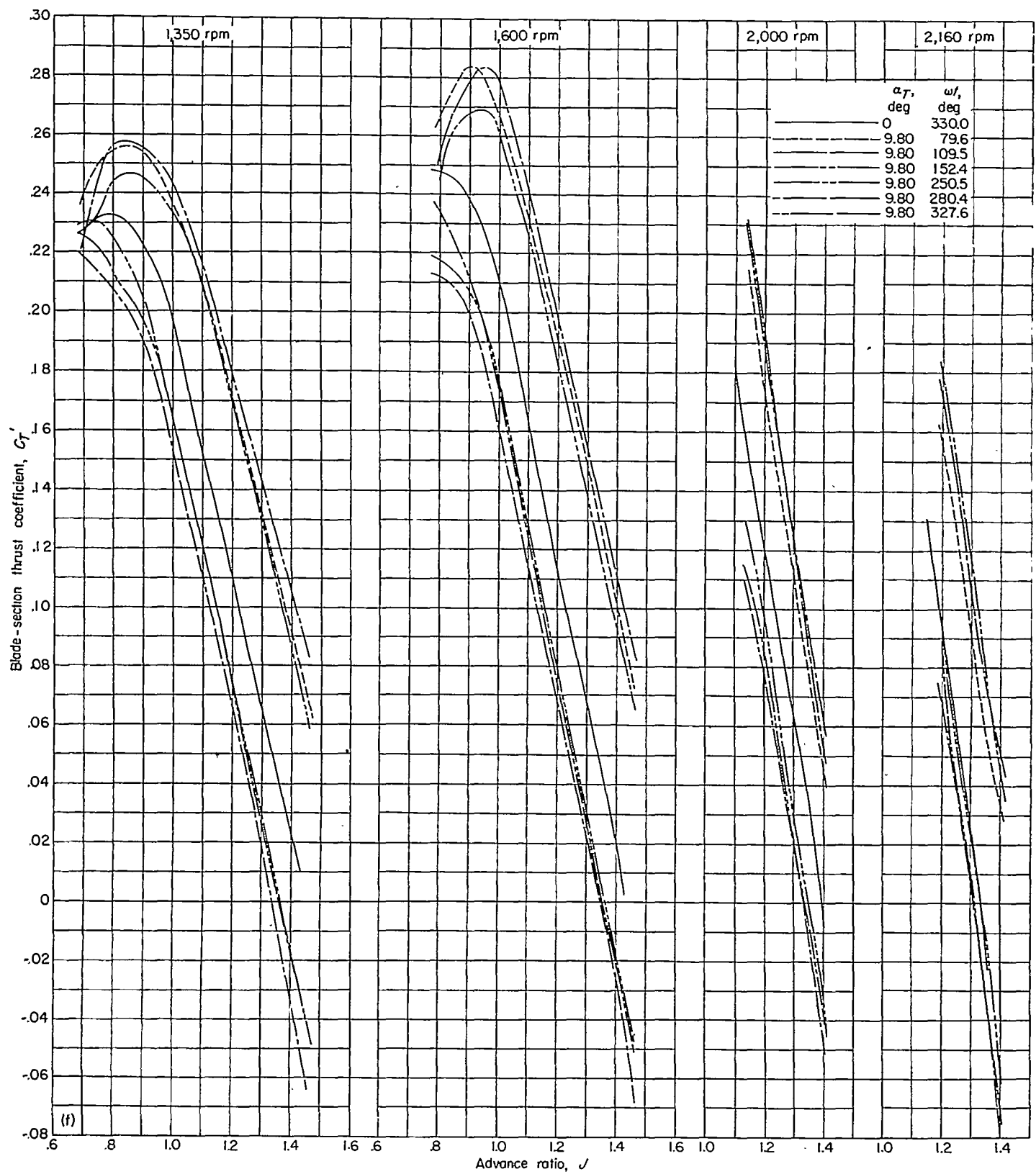
(f) $x=0.80$.

FIGURE 7.—Continued.
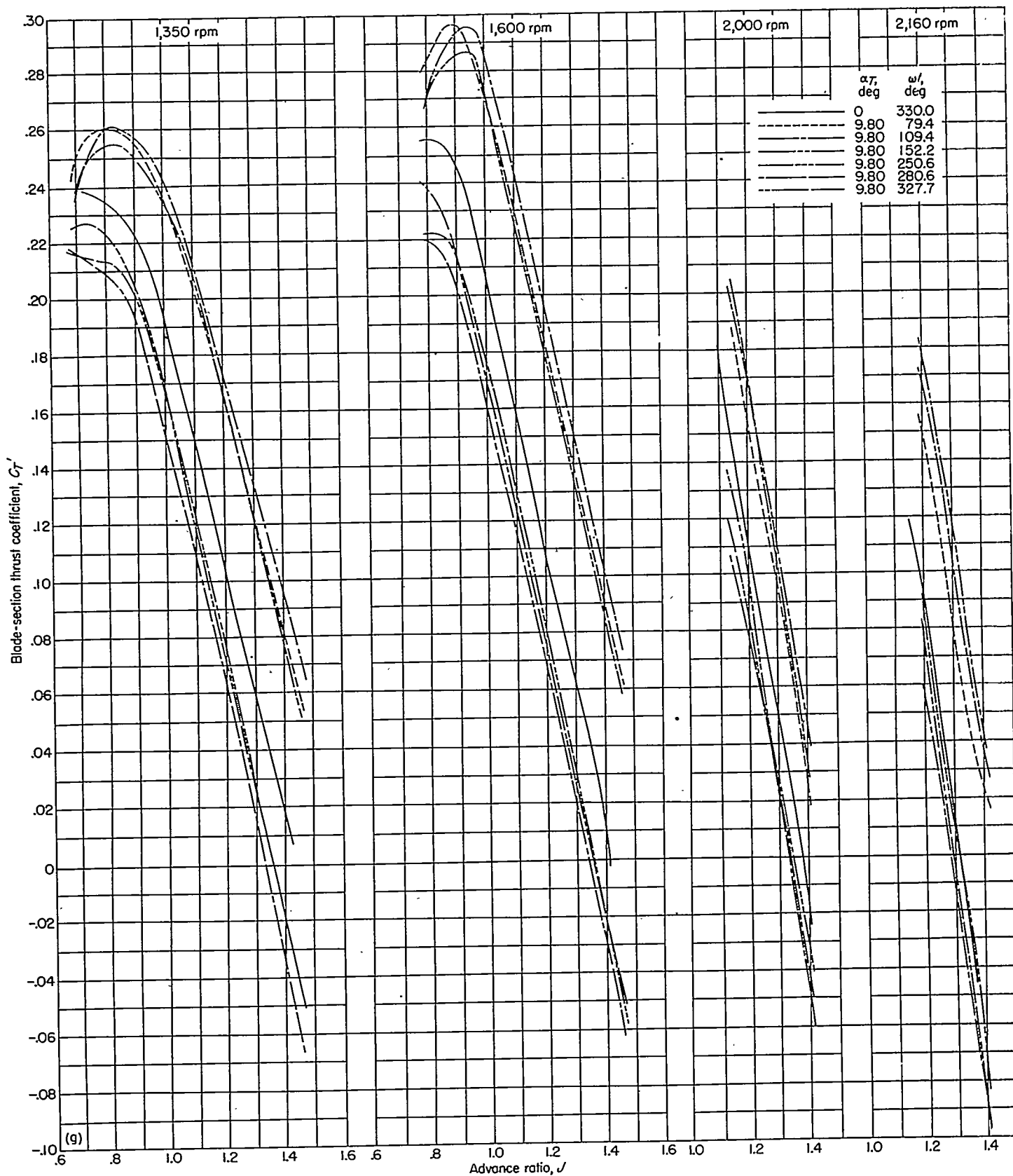
(g) $x = 0.85$.

FIGURE 7.—Continued.

(h) $x=0.90$.

FIGURE 7.—Continued.

α_T, deg	ω_l, deg
0	330.0
9.80	79.2
9.80	109.1
9.80	152.0
9.80	250.9
9.80	280.8
9.80	327.9
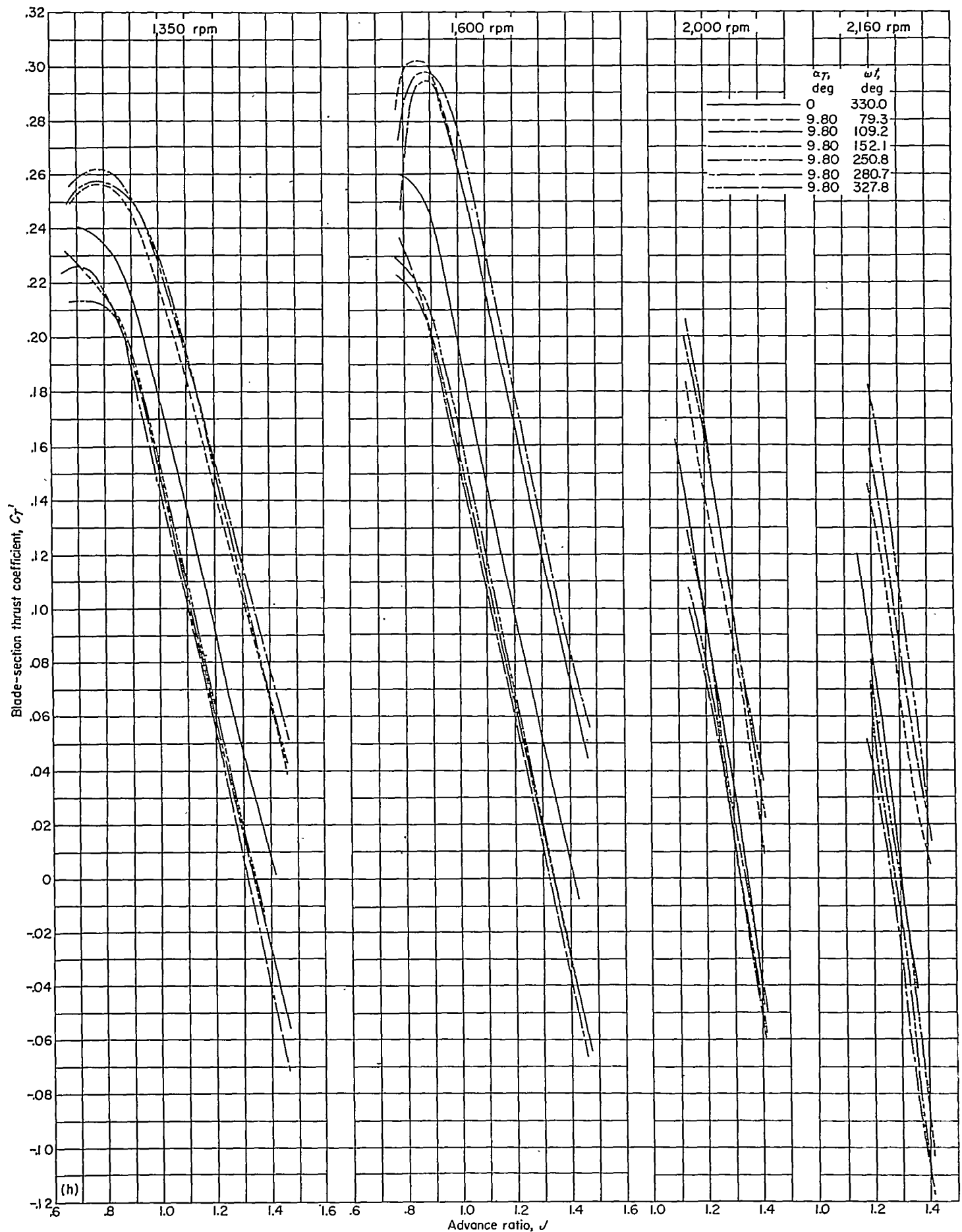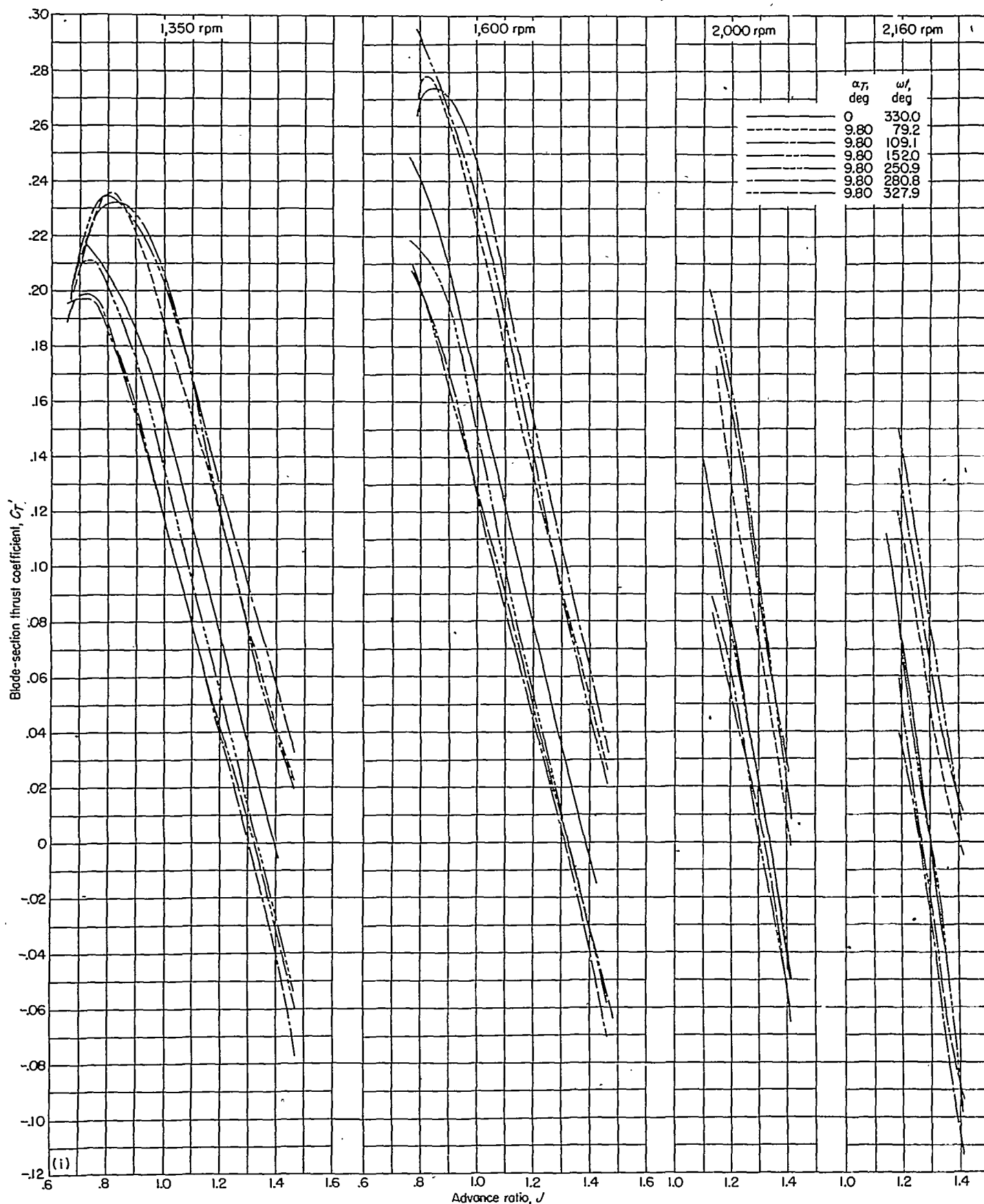
(i) $x=0.95$.

FIGURE 7.—Concluded.
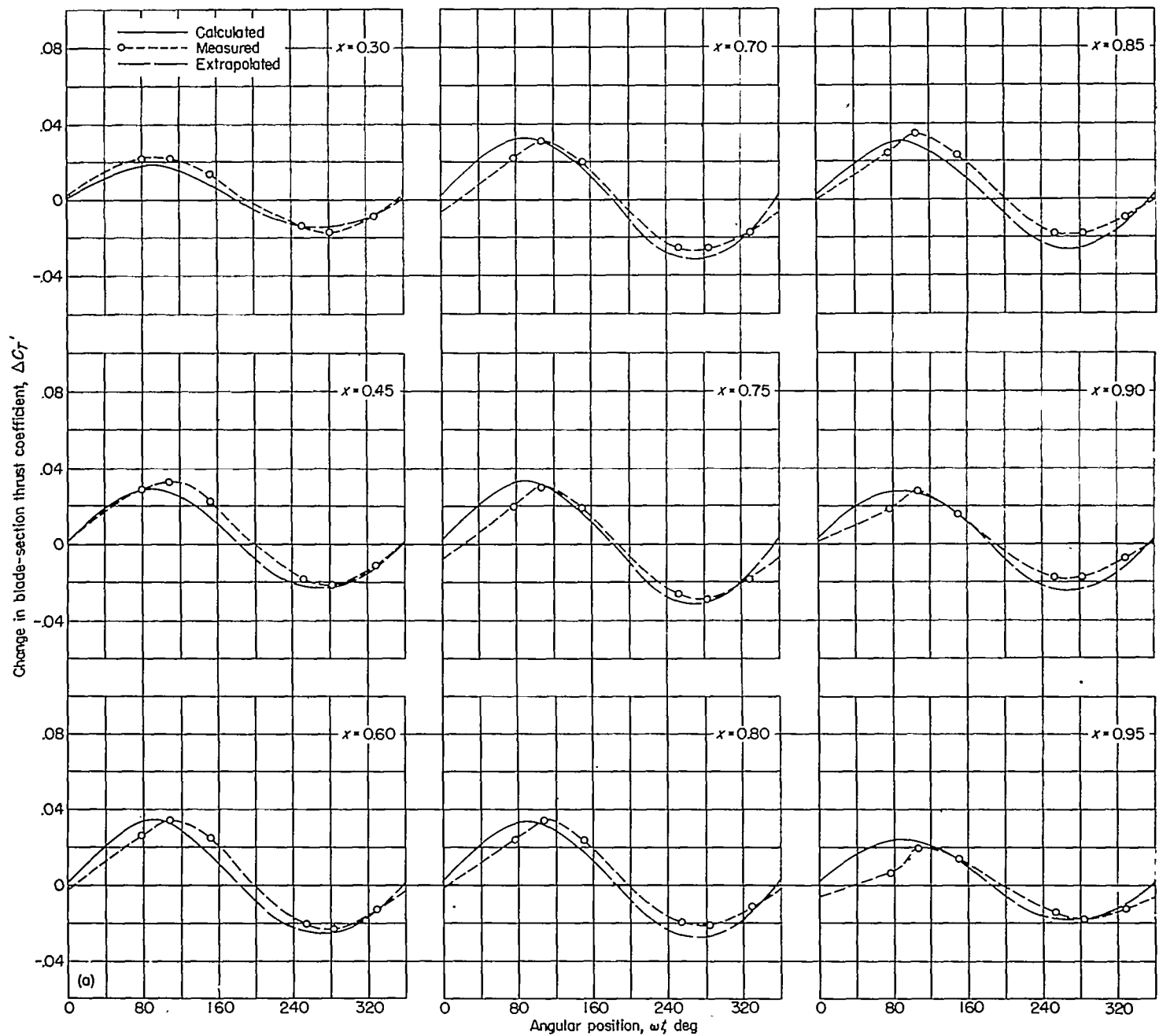
(a) $\alpha_T = 4.55°$; $N = 1,350$ rpm; $J = 1.2$.

FIGURE 8.—Change in blade-section thrust coefficient with angular position of blade.
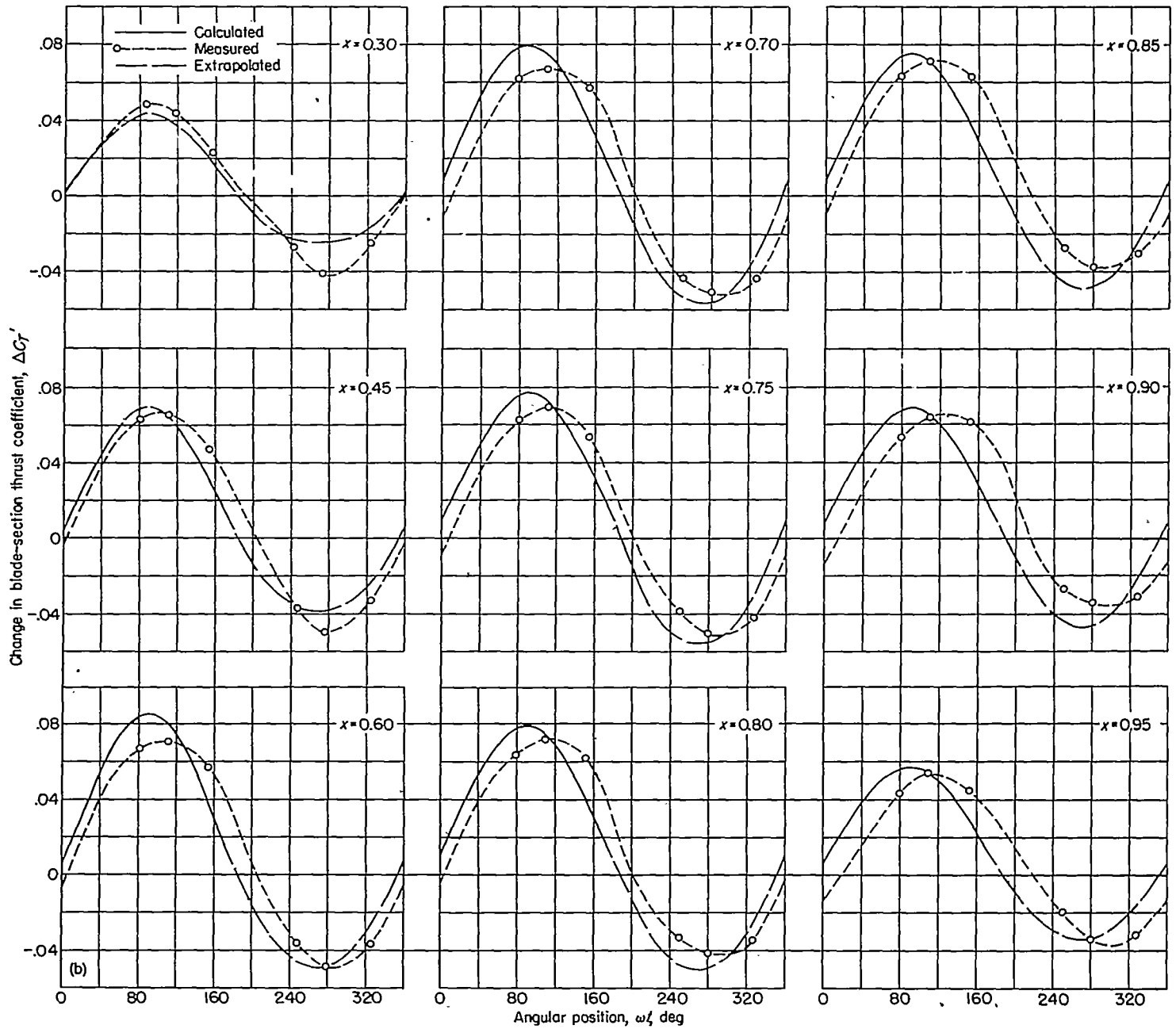
(b) $\alpha_T = 9.80°$; $N = 1,350$ rpm; $J = 1.2$.

FIGURE 8.—Continued.
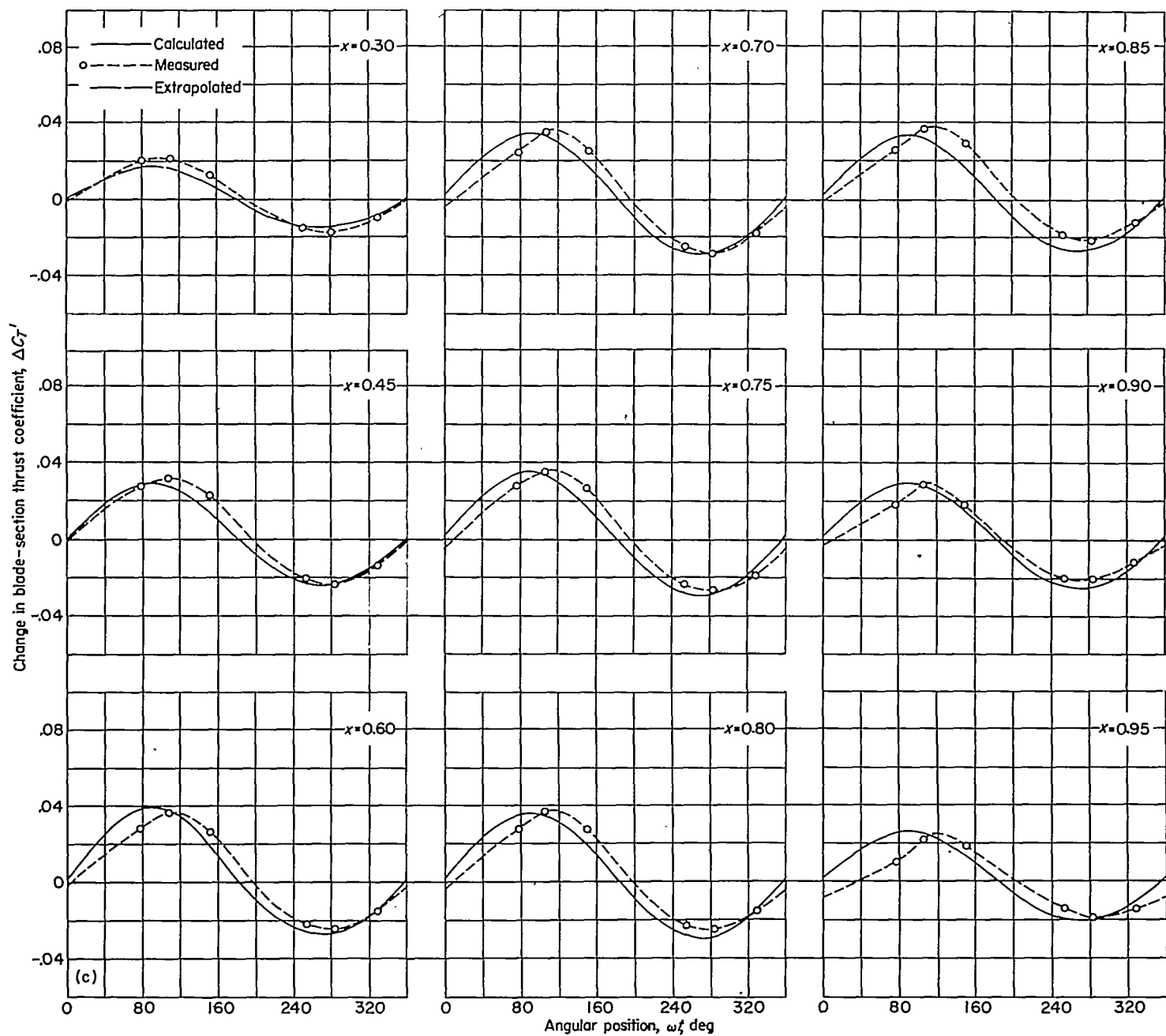
(c) $\alpha_T = 4.55°$; $N = 1,600$ rpm; $J = 1.2$.

FIGURE 8.—Continued.
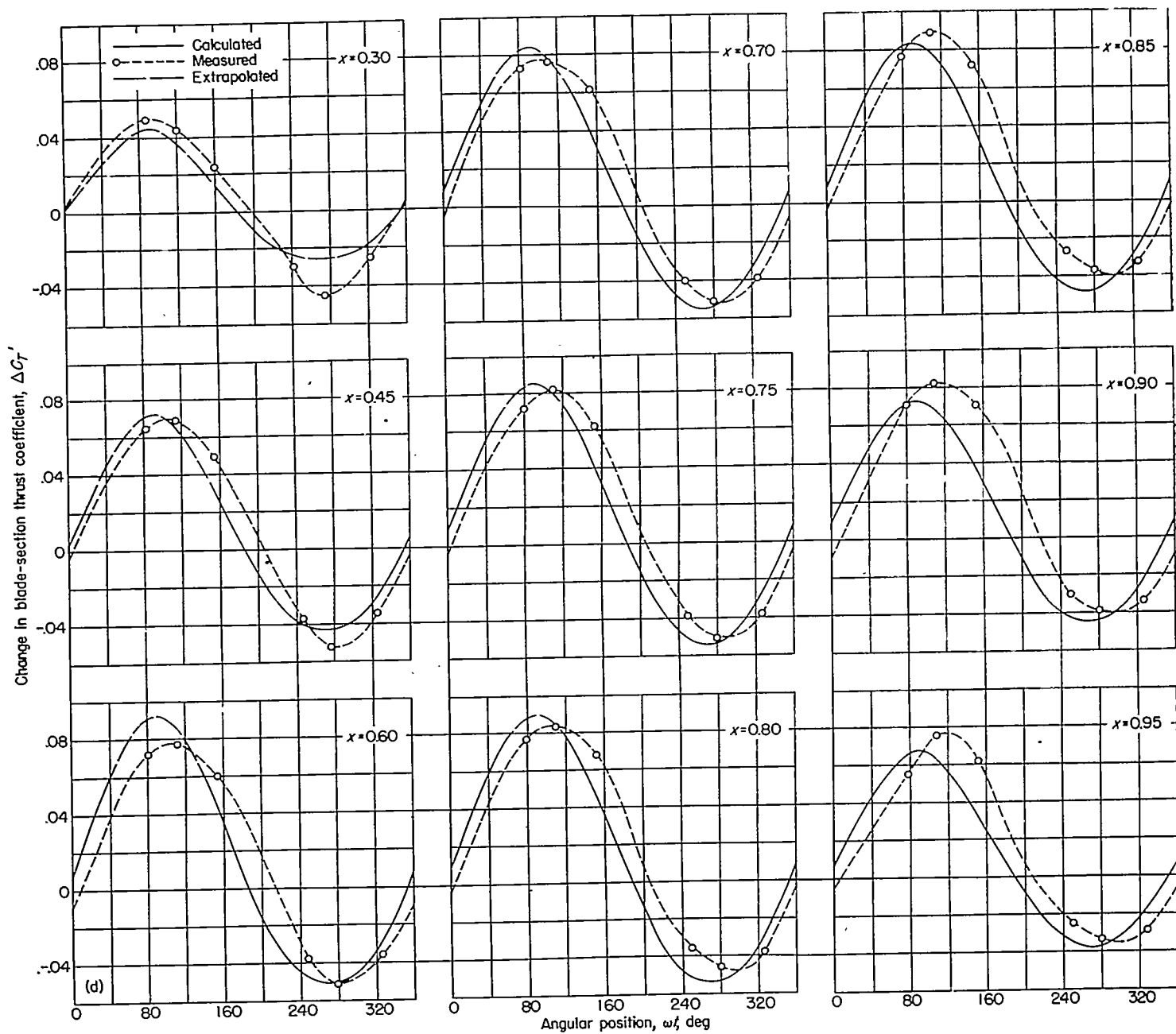
(d) $\alpha_T = 9.80°$; $N = 1,600$ rpm; $J = 1.2$.

FIGURE 8.—Continued.
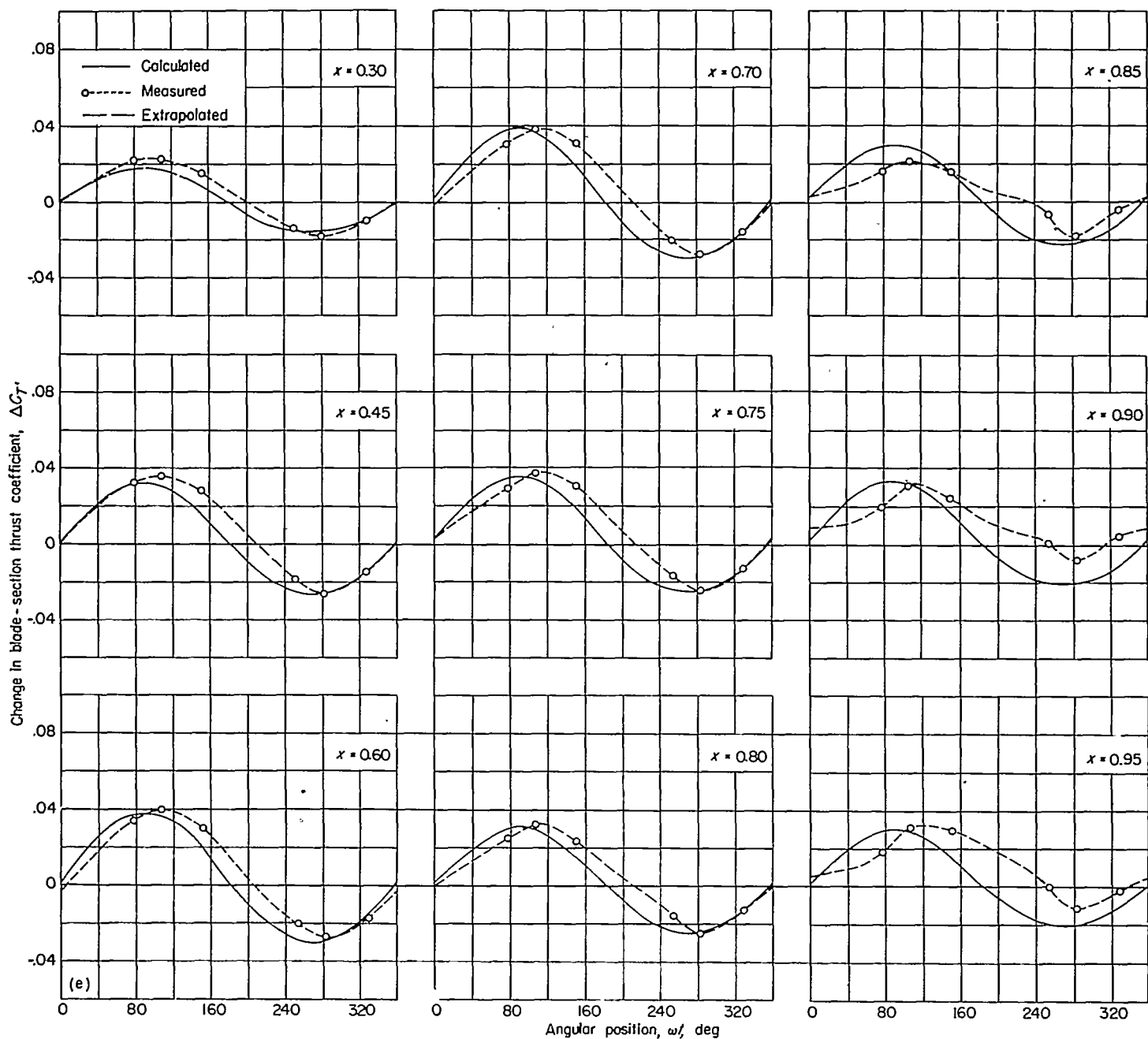
(e) $\alpha_T = 4.55°$; $N = 2,000$ rpm; $J = 1.25$.

FIGURE 8.—Continued.
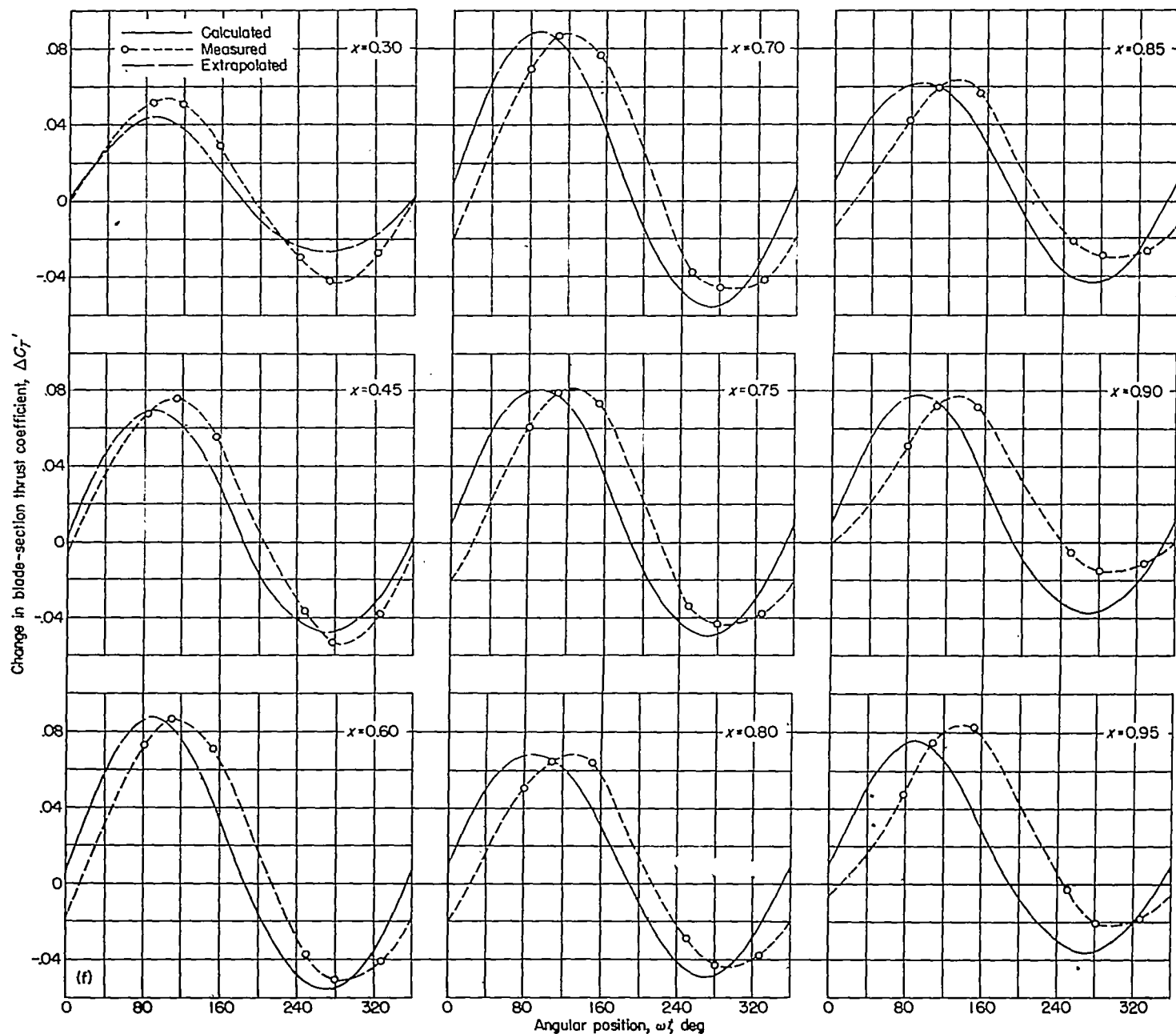
(f) $\alpha_T = 9.80°$; $N = 2,000$ rpm; $J = 1.25$.

FIGURE 8.—Continued.
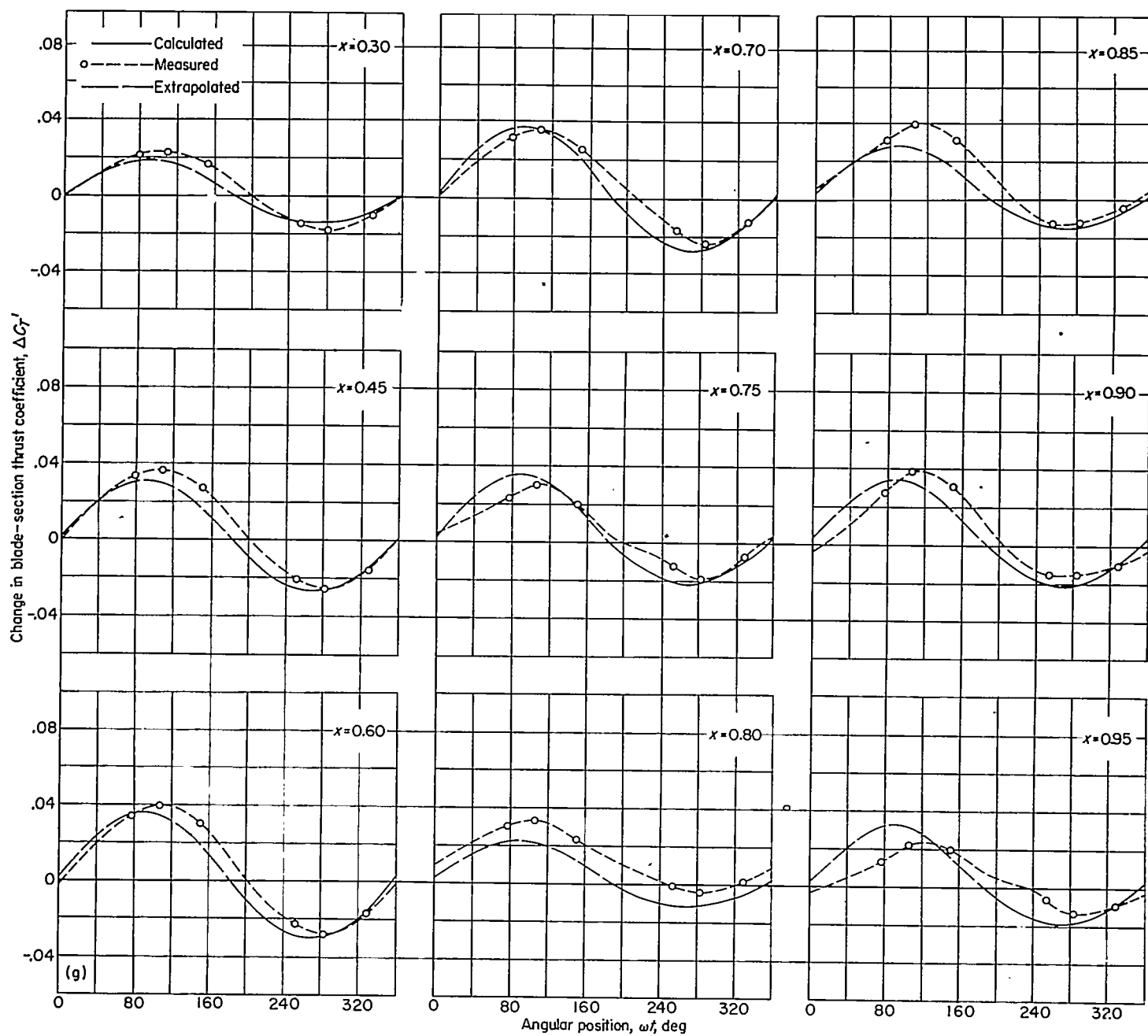
(g) $\alpha_T = 4.55°$; $N = 2,160$ rpm; $J = 1.25$.

FIGURE 8.—Concluded.
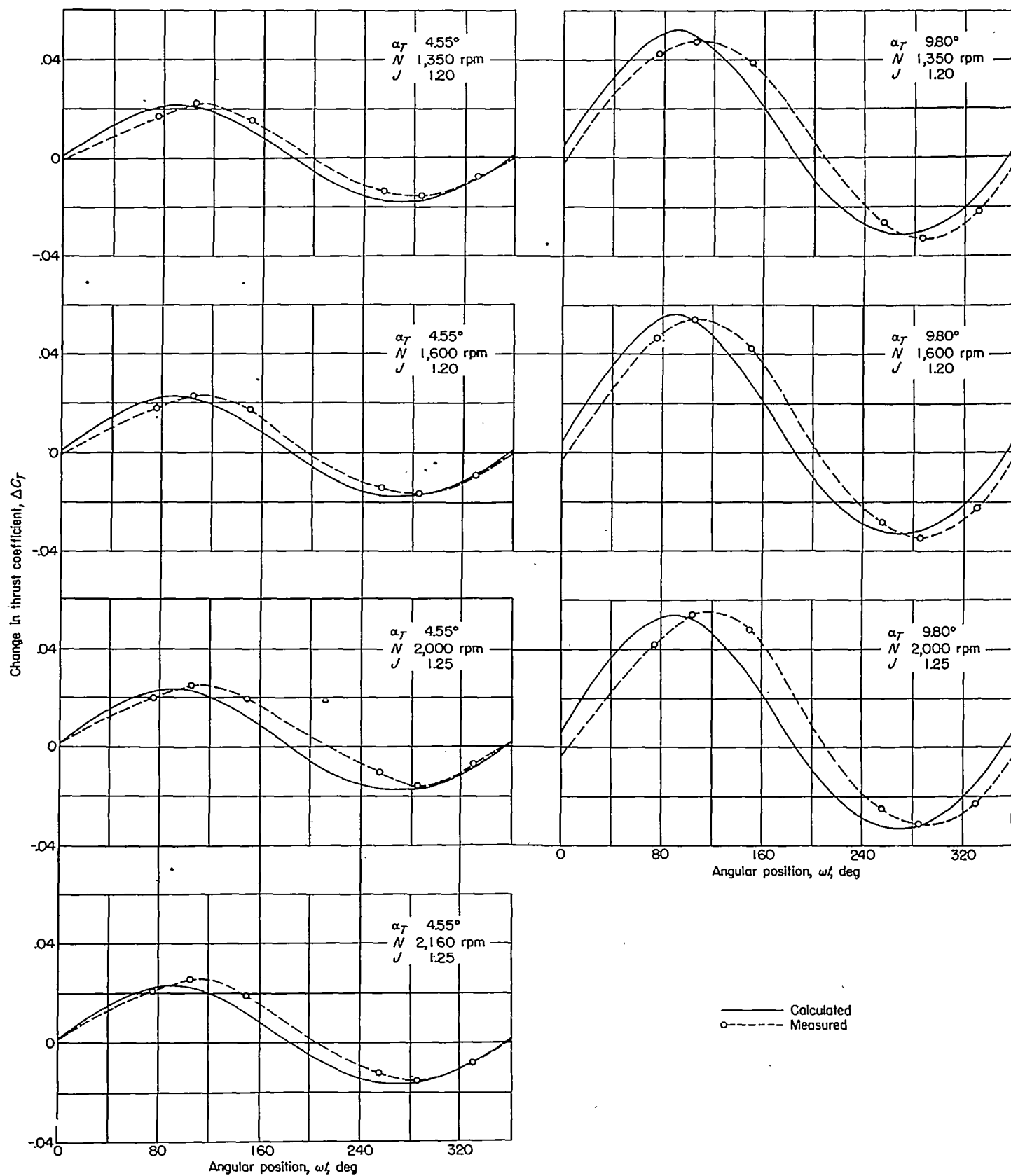
FIGURE 9.—Change in integrated thrust coefficient with angular position of blade.
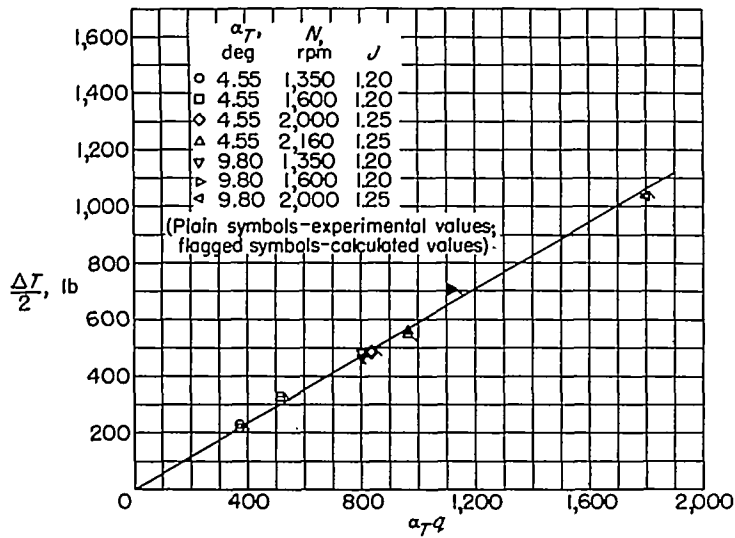
FIGURE 10.—Thrust variation as a function of the product $a_T q$.
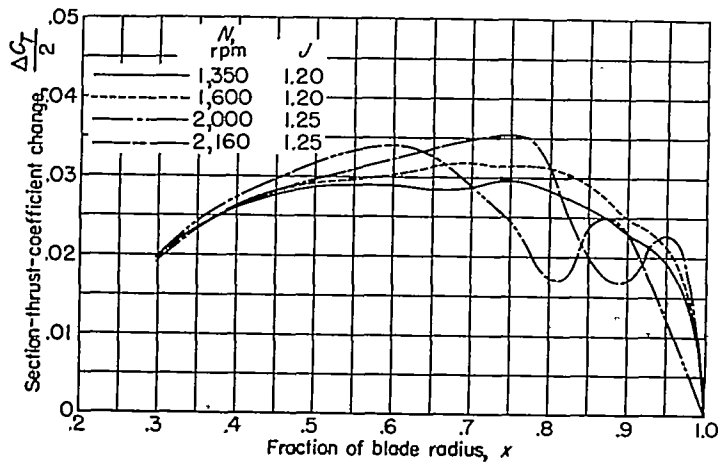
FIGURE 11.—Effect of rotational speed on change in section thrust coefficient for an inclination angle of 4.55°.
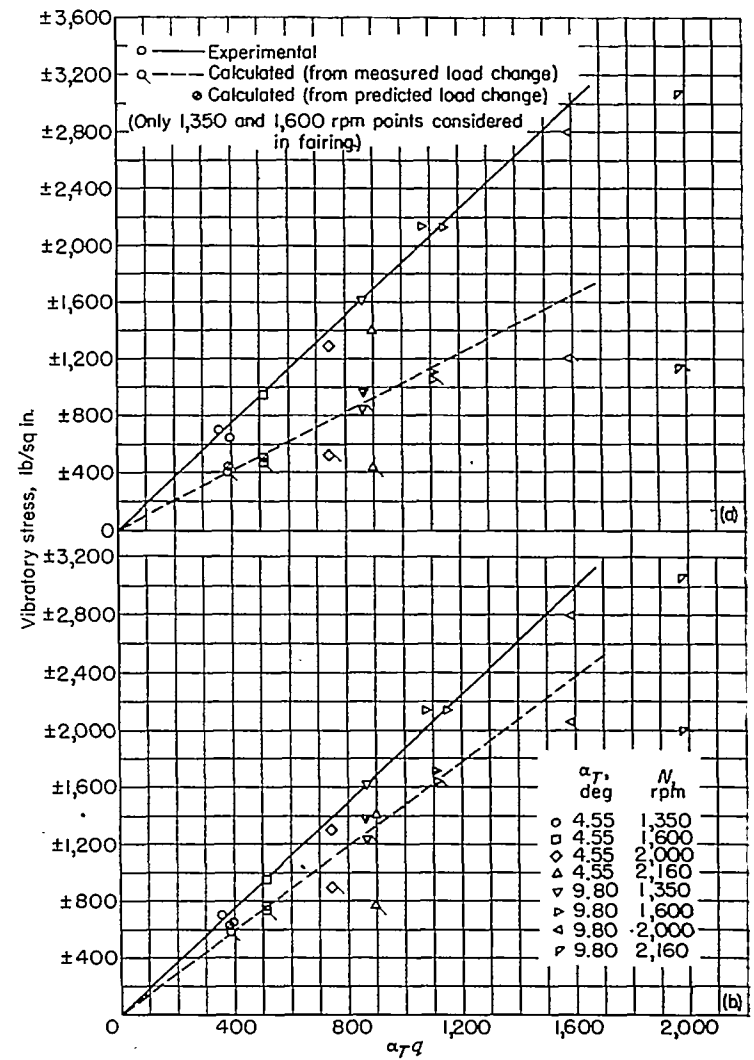
(a) Calculated values not corrected for resonance amplification.
(b) Calculated values corrected by estimated resonance amplification factor for first-order bending at propeller speed.
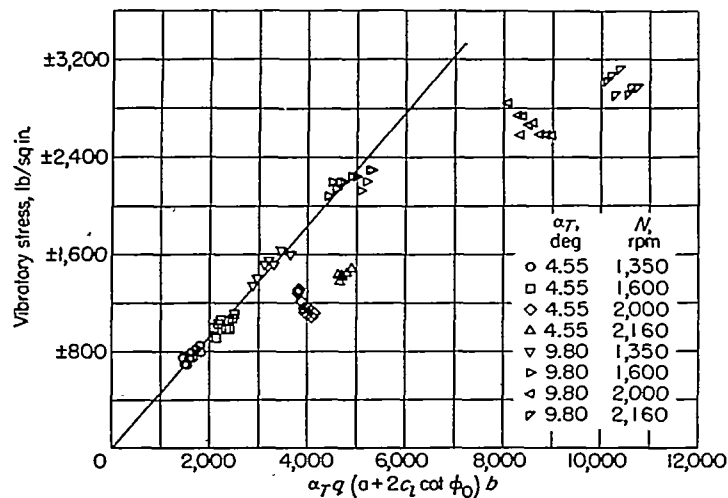
FIGURE 12.—Experimental and calculated stress comparison.

FIGURE 13.—Variation of vibratory stress with the product $\alpha_T q$ as modified for aerodynamic changes at $x=0.7$.
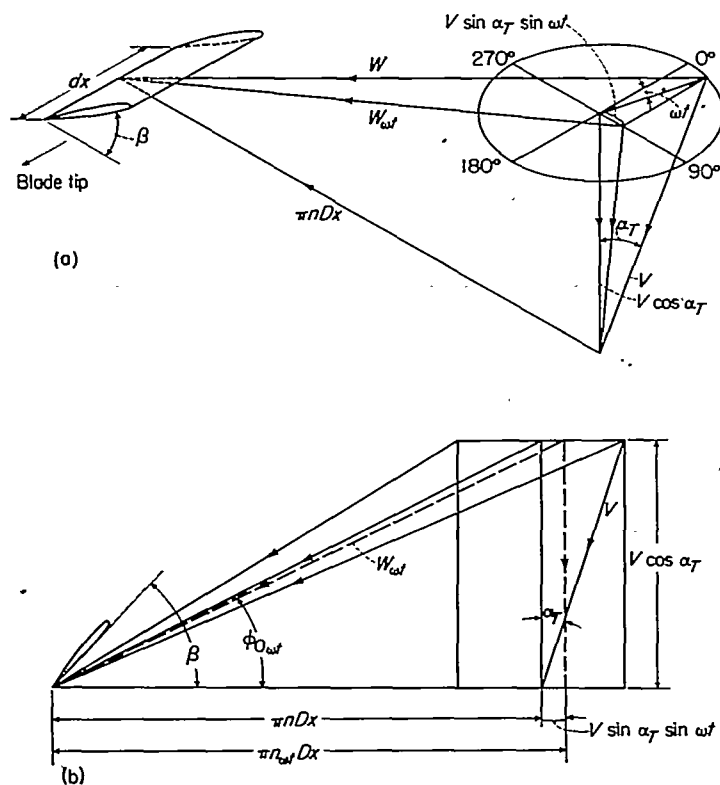

(a) Three-dimensional diagram.
(b) Diagram obtained by neglecting radial components of flow.

FIGURE 14.—Velocity diagrams for a propeller operating with its thrust axis inclined to the airstream.

(a) $x=0.30$.
(b) $x=0.45$.
(c) $x=0.60$.
(d) $x=0.70$.
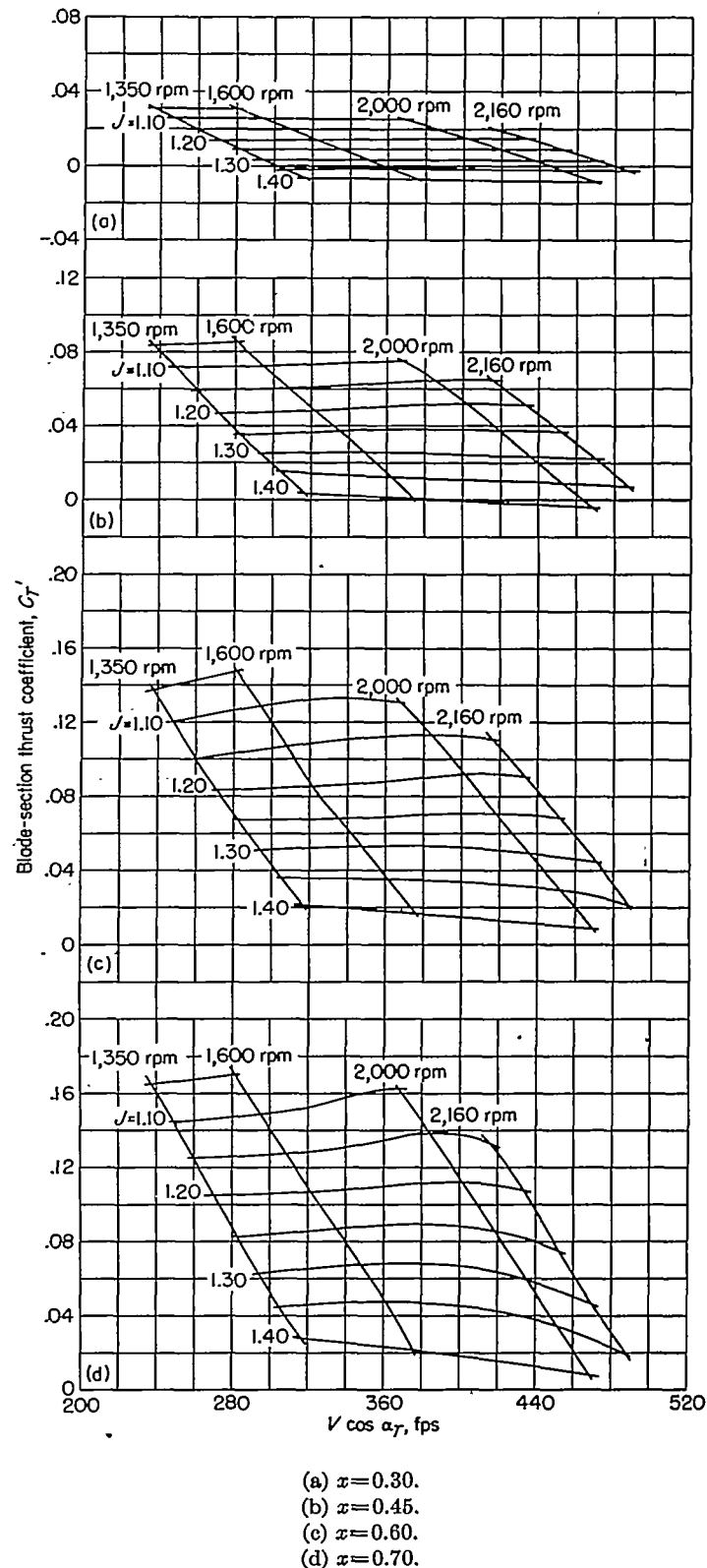
FIGURE 15.—Charts for estimating section thrust coefficients for an inclined three-blade 10–(3)(08)–03 propeller.
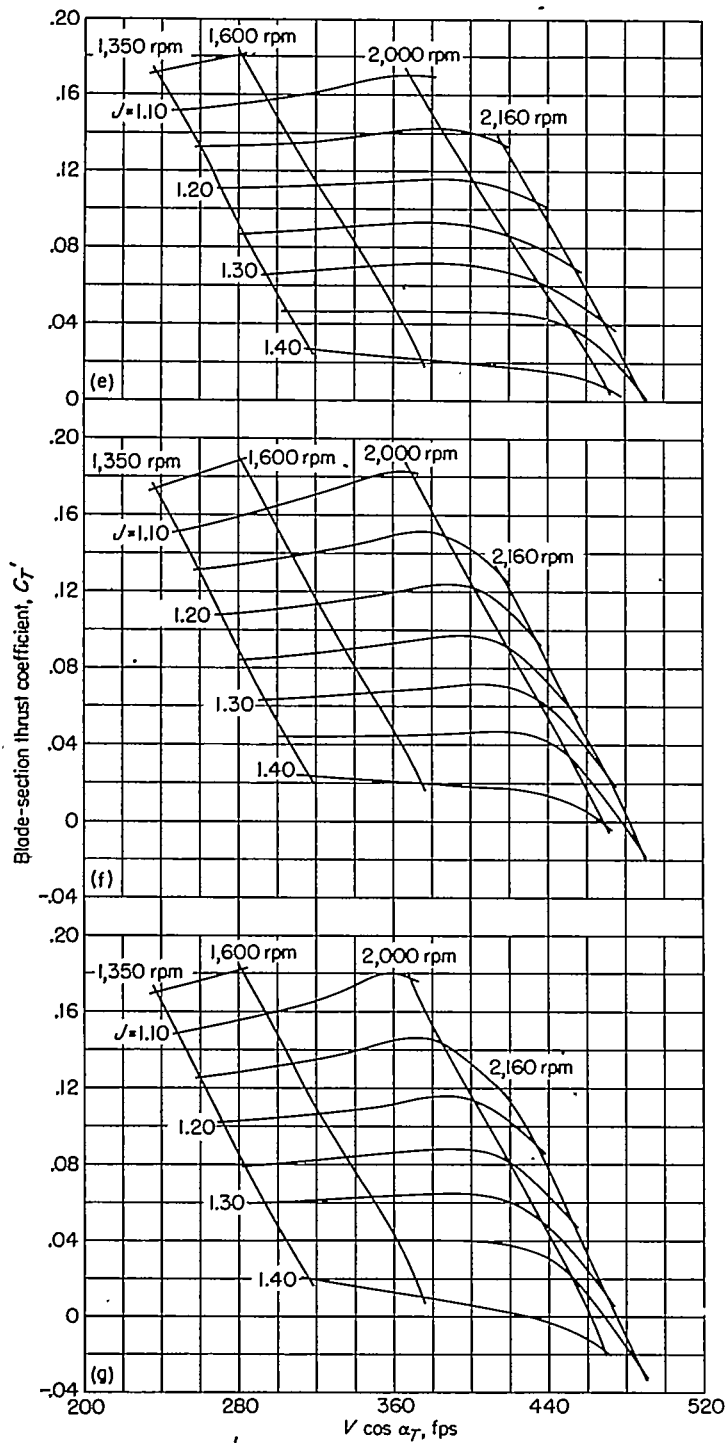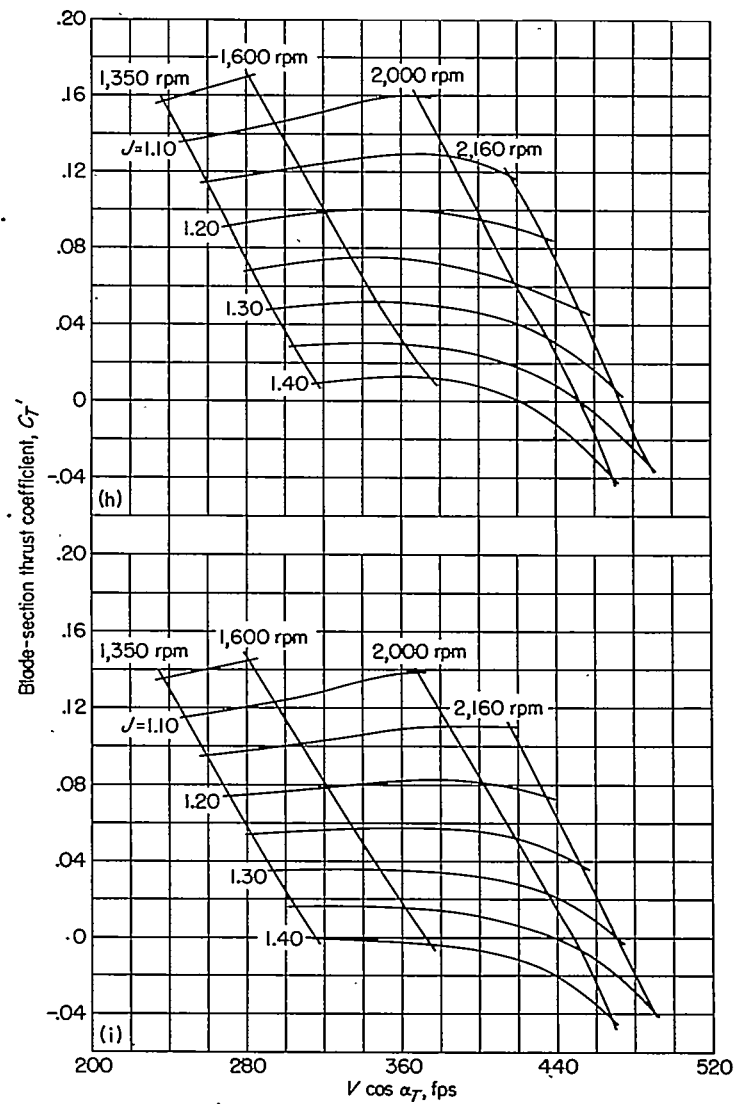
(e) x=0.75.
(f) x=0.80.
(g) x=0.85.
FIGURE 15.—Continued.

(h) x=0.90.
(i) x=0.95.
FIGURE 15.—Concluded.